# Sorption of Chlorinated Solvents in a Sandy Aquifer

by

## Crist Simon Khachikian

B.S., Civil and Environmental Engineering
University of California at Los Angeles, 1995

Submitted to the Department of Civil and Environmental Engineering
In Partial Fulfillment of the Requirements for the Degree of

MASTER OF ENGINEERING
in Civil and Environmental Engineering

at the

MASSACHUSETTS INSTITUTE OF TECHNOLOGY
June 1996

Signature of the Author _ ⎯⎯⎯⎯

Department of Civil and Environmental Engineering
May 15, 1996

Certifie

Philip M. Gschwend
Professor of Civil and Environmental Engineering
Thesis Supervisor

Accepted by ⎯⎯⎯⎯⎯⎯⎯⎯⎯⎯⎯⎯⎯⎯⎯⎯⎯⎯

Professor Joseph M. Sussman
Chairman, Departmental Committee on Graduate Studies

# Sorption of Chlorinated Solvents in a Sandy Aquifer

by

## CRIST S. KHACHIKIAN

Submitted to the Department of Civil and Environmental Engineering on
May 10, 1996 in partial fulfillment of the requirements for the degree of
Master of Engineering in Civil and Environmental Engineering

## *Abstract*

The sorptive uptake of hydrophobic organic chemicals by the sandy aquifer at Cape Cod, Massachusetts was studied. The use of theoretical sorption distribution coefficients was assessed by comparing these values to laboratory determined ones. Distribution coefficients were then used to understand the behavior of contaminants in the aquifer (i.e., bioavailability and dispersivity). The uptake of phenanthrene and pyrene by the aquifer sands at five depths (18-20', 58-60', 73-75', 78-80', and 88-90' below ground surface) was studied using a batch methodology. Even with the low organic carbon content of the sands (in general < 0.01%), association with that organic matter appeared to be the main route of solute uptake. Distribution coefficients obtained from the batch tests were in good agreement (within a factor of 0.6 to 1.2) with those obtained from theoretical relationships. With this in mind, theoretical distribution coefficients were calculated for dichloroethylene (DCE), trichlorothylene (TCE), and tetrachloroethylene (PCE). These were used to calculate retardation factors which were averaged over the sampling depth to obtain an aggregated effect. The averaged retardation factors were 1.04, 1.10, and 1.25 for DCE, TCE, and PCE, respectively. The bioavailability of these contaminants could be affected by retardation. Also, the retarded longitudinal macrodispersivity of each of these compounds increased over the conservative dispersivity by factors of 1.2 (DCE), 1.4 (TCE), and 2.1 (PCE).

The conclusions of this study are that site characterization efforts should be augmented to include sorption properties. In the absence of filed observations, theoretically derived distribution coefficients provide a convenient means by which to obtain distribution coefficients for many compounds. These properties are important in assessing the transport and transformations of contaminants in the subsurface and may significantly affect remedial schemes.

Thesis Supervisor : Dr. Philip M. Gschwend
                Title : Professor

# Acknowledgments

There have been many people who have been instrumental in helping me complete this work. This one year ordeal has been crazy, difficult, interesting, instructive, and, most of all, fun. Each of the following people contributed, in some part, to all of the above:

**Philip M. Gschwend** generously volunteered his time and helped me understand why I always have to ask why. His general state of excitement and, hopefully, some of his keen insight, have rubbed off on me. I am infinitely indebted to his advice, help, and generosity.

**Lynn Gelhar** patiently provided sound advice which helped me finish this work. His instructive approach to all my questions was refreshing and very helpful. He also obtained the sand samples used in this study from the USGS. Thanks to **Dennis LeBlanc** from the USGS who provided the samples.

The Gschwend lab has been an incredible environment to work in. The main reason for this was the people in the lab: **Örjan Gustafsson, John MacFarlane, Allison Mackay, Tom Ravens, Ken Motolenich-Salas, Chris Swartz,** and **Lukas Wick**. Special thanks to John who spent a lot of time with me during my "startup" time. Allison helped me with all the instruments in the lab and was always available for interesting conversations.

Outside of the laboratory, many others were an integral part of this past year. The M.Eng. program was well administered and organized by **David H. Marks** and **Shawn P. Morrissey**. Their positive and encouraging aura helped ease the anxieties and troubles of the past year. The students of the program provided an environment which I quite cant put my finger on yet. The wide range of personalities, beliefs, and backgrounds provided for an interesting learning experience. Special thanks to my group mates **Beto Lázaro, Enrique "Chicharonero" López-Calva, Tintin Picazo, Pete Skiadas, and Donald Tillman**. The many late nights, heated fights, and greasy pizzas we shared will never be forgotten.

Last, but not least, there is a special group of people I would like to thank. We were separated physically but they have been with me throughout this year. My mother **Seda**, sister **Annie**, and father **Hartun** consistently provided love, support, and encouragement and served as a sanity check from time to time. Finally, my partner in life, **Tina Salmassi**, was a source of infinite love, support, amusement, and dumb email jokes. Without her I would have never accomplished what I have so far. Without her by my side I do not plan to accomplish much in the future.

# Table of Contents

# List of Tables

# List of Figures

# 1. Introduction

This thesis deals with the sorption of chlorinated solvents in a sandy aquifer. The aquifer studied is that underlying the Massachusetts Military Reservation (MMR), Cape Cod, Massachusetts. This aquifer is contaminated by many contaminant plumes emanating from the MMR. One of these plumes, Chemical Spill 4 (CS-4) was singled out for this study. The contaminants of concern in CS-4 are *cis*-1,2-dichloroethene (*c*-DCE), *trans*-1,2-dichloroethene (*t*-DCE), trichloroethene (TCE), and tetrachloroethene (PCE). This thesis constitutes one part of a project with is a conglomeration of six different theses. Each of the theses dissects a particular aspect of CS-4. The project contributes to an understanding of the plume and presents a final remedial scheme for restoring the aquifer to federally accepted clean levels. The fourth and fifth chapters present the bulk of the work for this thesis. The appendix includes the results of the group project report which includes information on the migration of the plume, schemes for its containment, and a proposed remedial action. For more detailed information on the other theses, the reader is referred to Lázaro (1996), López-Calva (1996), Picazo (1996), Skiadas (1996), and Tillman (1996).

## 1.1 Problem

The Cape Cod aquifer is contaminated by various pollutants emanating from the Massachusetts Military Reservation (MMR). One such plume of contaminants, termed CS-4, is presently being contained. A pump and treat system has been installed to prevent the advancement of the plume. Contaminated water is extracted at the toe of the plume, treated to reduce the contaminant concentrations to federal maximum contaminant levels, and discharged back to the aquifer. However, this pump and treat system is an expensive interim remedial action. A final remedial plan must be formulated to completely clean up the groundwater. Sorption plays an important role in the understanding the fate and transport of contaminants and may significantly affect remediation schemes.

## 1.2 Objectives

The objectives of this study were to understand the sorptive capacity of the sandy aquifer at Cape Cod. Sorption is an integral part of the site characterization process and is important in the transport of the contaminants since it may affect contaminant travel velocity and dispersivity. Also, pump and treat and bioremediation schemes, as the ones reported in the appendices, can be significantly affected by sorption. To this end, this study tries to answer the following questions:

1. Can theoretical distribution coefficients be used to assess the sorptive uptake of contaminants for sediments with low levels of organic carbon?

2. How much sorptive uptake can be expected by the aquifer sediments?

3. How does sorption affect the transport of the contaminants?

4. How does the bioavailability of the contaminants change because of sorption?

## 1.3 Scope

The sorptive capacity of the sandy aquifer at Cape Cod, Massachusetts is studied here. Equilibrium sorption distribution coefficients were used to assess the behavior of a contaminant plume consisting of DCE, TCE, and PCE. Sorption kinetics was studied to assess the attainment of equilibrium conditions in the laboratory. The assumption of equilibrium sorption and the use of equilibrium sorption coefficients is discussed.

Section 2 includes a brief description of the site. This chapter is included to orient the reader with the location, physical description, history, and current remedial situation at Cape Cod.

Section 3 provides a fairly detailed site characterization which was mainly extracted from many studies conducted at Cape Cod. Included here are the geology, the hydrology, and the hydrogeology of Cape Cod.

Section 4 includes a brief theory on equilibrium sorption. Theoretical distribution coefficients are introduced and calculated in this section.

The results of the laboratory batch tests are included in section 5. Here, the methodology used for the batch tests is outlined. The experimental distribution coefficients are included here and are related to the theoretical values obtained in section 4.

Finally, the conclusions and recommendations are included in section 6.

# 2. Site Description

## 2.1 *Location*

Cape Cod is located in the southeasternmost point of the Commonwealth of Massachusetts (Figure 2-1). It is surrounded by Cape Cod Bay on the north, Buzzards Bay on the west, Nantucket Sound to the south, and the Atlantic Ocean to the east. Cape Cod, a peninsula, is separated from the rest of Massachusetts by the man-made Cape Cod Canal.
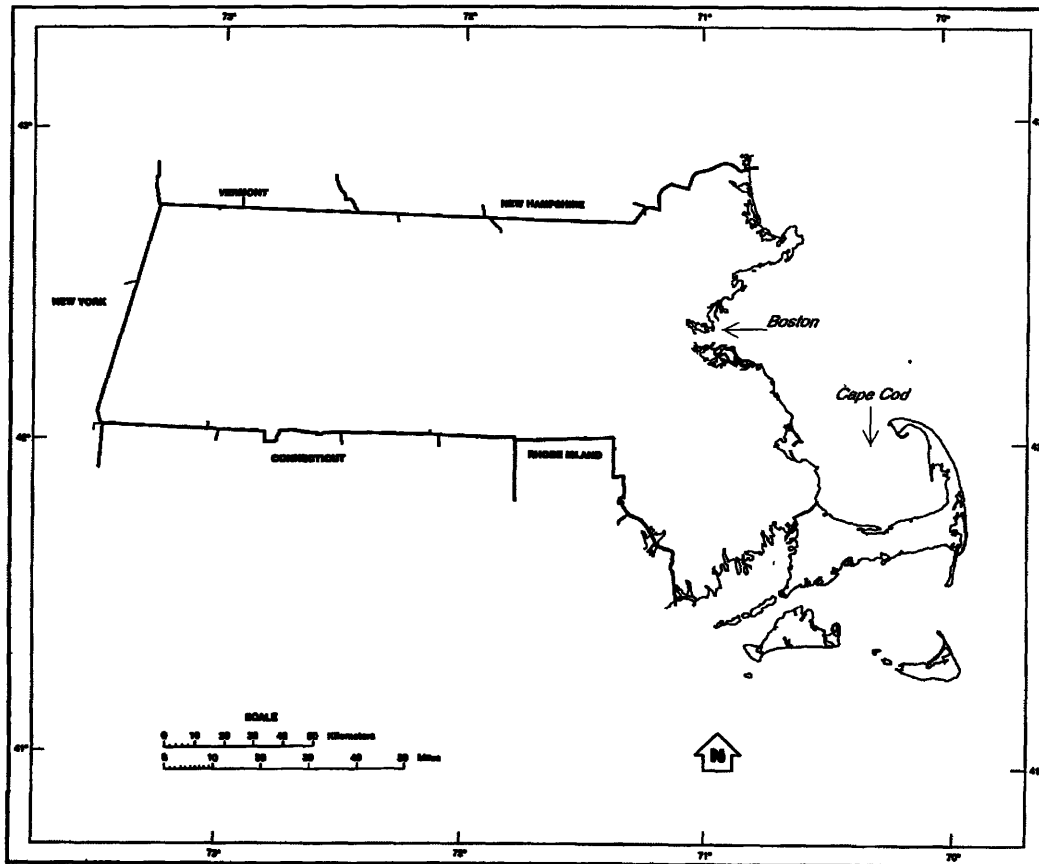
Figure 2-1: Map of the Commonwealth of Massachusetts

The MMR is situated in the northern part of western Cape Cod (Figure 2-2). Previously known as the Otis Air Force Base, the MMR occupies an area of approximately 22,000 acres (30 square miles).
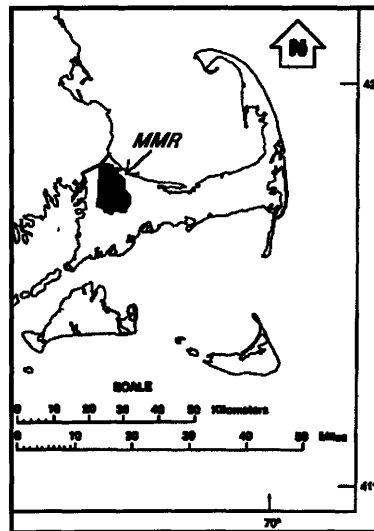


Figure 2-2. Location of MMR

## 2.2 General Physical Site Description

Cape Cod sediments are predominantly composed of sand and gravel with a low percentage of silt. Left behind by the advancement of a glacier thousands of years ago, these deposits are generally well-sorted, but layered, and therefore heterogeneous in character. The origin and nature of the deposits has results in a low fraction of organic carbon in the sediments. These sandy deposits allow a large portion of precipitation to seep beneath the surface into groundwater aquifers. This is the only form of recharge these aquifers receive. The groundwater system of Cape Cod serves as the only source of drinking water for most residents.

## 2.3 Land and Water Use

Water covers over 4% of the surface area of Cape Cod. This water is distributed among wetlands, kettle hole ponds, cranberry bogs, and rivers. Nevertheless, all 15 communities meet their public supply needs with groundwater. Individual towns develop and maintain separate municipal water supply systems. Falmouth is the only municipality that uses some surface water (from the Long Pond Reservoir) as a source of drinking water. Approximately 75% of the Cape's residents use water supplied through public works, while the remaining use private wells within their property. Because of the heavy dependence on groundwater as a drinking water source, the protection of this resource is of paramount concern.

Water work agencies are called to supply twice as much water during the summer months than during the off-season (September through May). The highest monthly average daily demand (ADD) in 1990 was in July when 34.98 mgd were used. The lowest monthly ADD was in February with 14.03 mgd (Massachusetts Executive Office of Environmental Affairs, 1994).

## 2.4 MMR Setting and History

The MMR has been used for military purposes since 1911. From 1911 to 1935, the Massachusetts National Guard periodically camped, conducted maneuvers, and pursued weapons training in the Shawme Crowell State Forest. In 1935, the Commonwealth of Massachusetts purchased the area and established permanent training facilities. Most of the activity at the MMR occurred after 1935, including operations by the U.S. Army, U.S. Navy, U.S. Air Force, U.S. Coast Guard, Massachusetts Army National Guard, Air National Guard, and the Veterans Administration.

The majority of the activities consisted of mechanized army training and maneuvers as well as military aircraft operations. These operations inevitably included the maintenance and support of military vehicles and aircraft. The level of activity has greatly varied over the MMR operational years. The onset of World War II and the demobilization period following the war (1940-1946) were the periods of most intensive army activity. The period from 1955 to 1973 saw the most intensive aircraft operations. Today, both army training and aircraft activity continue at the MMR, along with U.S. Coast Guard activities. However, the greatest potential for the release of contaminants into the environment was between 1940 and 1973. Wastes generated from these activities may include oils, solvents, antifreeze, battery electrolytes, paint, waste fuels, and metals and dielectric fluids from transformers and electrical equipment (E.C. Jordan, 1989b).

## 2.5 Current Situation

### 2.5.1 Interim Remedial Action and Objectives for Final Remedy

The existing remedial action was designed as an interim solution, with the objective of containing the plume against further migration. This was achieved by placing pumping wells at the plume toe and treating the extracted water (Figure 2-3).
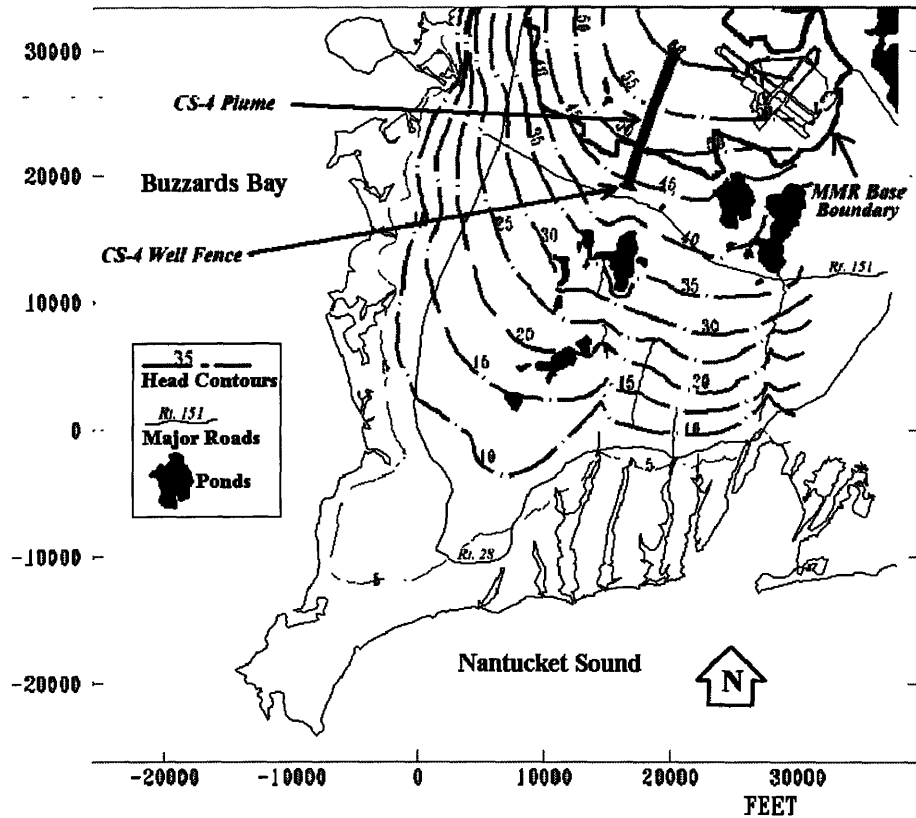
Figure 2-3. CS-4 plume and well-fence location

In contrast, a final remedial action will address the overall, long-term objectives for the CS-4 Groundwater Operable Unit. In terms of treatment objectives, the target levels for the treated water are defined through the established Maximum Contaminant Levels (MCL) (Table 2-1). Maximum measured concentrations, average concentrations within the plume, and an approximate frequency of detection are also included in Table 2-1. Although the existing remedial action is interim, its clean-up goals have to be consistent with the long-term goals. Therefore, the target levels in Table 2-1 are also applicable to the existing interim action.

15

Table 2-1. Concentrations of contaminants of concern and treatment target levels (adapted from ABB Environmental Services, Inc., 1992b).

| Contaminant of concern | Maximum Concentration (ppb) | Average Concentration (ppb) | Frequency of detection | MCL (ppb) |
|---|---|---|---|---|
| Tetrachloroethene (PCE) | 62 | 18 | 14/20 | 5 |
| Trichloroethene (TCE) | 32 | 9.1 | 14/20 | 5 |
| Total 1,2-Dichloroethene(DCE) | 26 | 1.1 | 11/20 | 70 |
| 1,1,2,2-Tetrachloroethane TeCA | 24 | 6.8 | 1/20 | 2[a] |

[a]No Federal or Massachusetts limits exist. Therefore, a risk-based treatment level was proposed. This was calculated assuming a $1 \times 10^{-5}$ risk level and using the USEPA risk guidance for human health exposure scenarios.

## 2.5.2 Existing Remedial Action

The currently operating remediation system consists of the following components:

- Extraction of the contaminated groundwater at the leading edge of the plume by 13 adjacent extraction wells.

- Transport of the extracted water to the treatment facility at the edge of the MMR area.

- Treatment of the water with a granular activated carbon system.

- Discharge of the treated water back into the aquifer to an infiltration gallery next to the treatment facility.

The treatment facility consists of two adsorber vessels in series filled with granular activated carbon (GAC). This system of two downflow, fixed-bed adsorbers in series is one of the most simple and widely utilized design for groundwater treatment applications (Stenzel et al., 1989). Two vessels in series assures that the carbon in the first vessel is completely exhausted before it is replaced, thus contributing to the overall carbon

efficiency. The removed carbon is transported off-site for reactivation.

## 2.5.3 Plume Location

The CS-4 plume is located in the southern part of MMR and is moving southward (Figure 2-3). From field observations, the dimensions of the plume have been defined as 11,000 ft in length, 800 ft wide and 50 ft thick (E.C. Jordan, 1990). According to these dimensions the volume of the plume is estimated to be 4 x $10^9$ L. Using the average concentrations of the contaminants (Table 2-1), the total volumes of contaminants in the groundwater are estimated to be about 40 L for PCE, 20 L for TCE, and 5 L for total DCE.

## 2.5.4 Performance of Current Remediation Scheme

The current treatment facility started operating in November 1993. Since then, only minimal inflow concentrations of 0.5 ppb have been detected and treated (ABB Environmental Services, Inc., 1996).

Numerous authors have raised serious concerns about the ability of existing pump and treat to restore contaminated groundwater to sound environmental and health-based sound standards (Mackay and Cherry, 1989; Travis and Doty 1990; MacDonald and Kavanaugh, 1994). Other studies have shown that pump and treat in conjunction with other treatment technologies can restore aquifers effectively (Ahlfeld and Sawyer, 1990; Bartow and Davenport, 1995; Hoffman, 1993). However, there is a consensus that pump and treat is an effective means of *controlling* the plume migration.

In conclusion, the interim CS-4 pump and treat system seems to be appropriate way to quickly respond to the plume migration. However, for the final CS-4 remedial system new methods of remediating the aquifer must be addressed. To this end, this report examines the role of sorption in the understanding of the plume fate and transport. Also, the effects of sorption on the remediation schemes are discussed.

# 3. Site Characterization

The site characterization presented here is a review of the literature concerned with Cape Cod. It is presented here to orient the reader with the general aquifer properties. It is important to understand the complete picture of the site so that the role and implications of sorption can be fully ascertained.

## 3.1 Geology

The geology of western Cape Cod is composed predominantly by glacial sediments deposited during the Wisconsin Period (7,000 to 85,000 years ago) (E.C. Jordan, 1989b). The three predominant geologic formations of the western Cape are the Sandwich Moraine (SM), the Buzzards Bay Moraine (BBM), and the Mashpee Pitted Plain (MPP) (E.C. Jordan, 1989b). The two moraines were deposited by the glacier along the northern and western edges of western Cape Cod. Between the two moraines lies a broad outwash plain (the MPP) which is composed of well sorted, fine to coarse-grained sands. At the base of unconsolidated sediments (below the MPP), fine grained, glaciolacustrine sediment and basal till are present.

Both the outwash and the moraines have relatively uniform characteristics at the regional scale, even though they contain some local variability. The sediments are stratified and thus the hydraulic conductivities are anisotropic. The MPP is more permeable and has a more uniform grain size distribution than the moraines (E.C. Jordan, 1989b).

The total thickness of the unconsolidated sediments (i.e., moraine, outwash, lacustrine, and basal till) is estimated to increase from approximately 175 feet near the Cape Cod Canal in the northwest to approximately 325 feet in its thickest portion in the BBM; it then decreases to 250 feet near Nantucket Sound in south. The thickness of the MPP outwash sediments ranges from approximately 225 feet near the moraines, to approximately 100 feet near shore of Nantucket Sound (E.C. Jordan, 1989a).

19

## 3.2 Hydrology

Cape Cod's temperate climate produces an average annual precipitation of about 48 inches, widely distributed throughout the year (Masterson and Barlow, 1994). High permeability sands and low topographic gradient, minimize the potential for runoff and erosion, and thus recharge values have been reported in the range of 17 to 23 inches/year (LeBlanc et al., 1986). Consequently, about one half of the water that precipitates recharges the aquifer. This creates a high probability of contaminant transport from the surface to the groundwater.

Beneath western Cape Cod lies a single groundwater system (from the Cape Cod Canal to Barnstable and Hyannis) which the U.S. Environmental Protection Agency (EPA) has designated as a sole source aquifer (E.C. Jordan, 1990). This aquifer is unconfined and its only form of natural recharge is by infiltration from precipitation. The highest point of the water table (the top of the groundwater mound) is located beneath the northern portion of the MMR. In general, groundwater flows radially outward from this mound and ultimately discharges to the ocean.

Kettle hole ponds, depressions of the land surface below the water table, are common on the MPP. These ponds influence the groundwater flow on a local scale. Streams, wetlands and cranberry bogs serve as drainage for some of these ponds and as areas of groundwater discharge, and thus comprise the rest of the hydrology of the western Cape. Figure 2-3 shows some hydrologic features (for example, ponds, water table elevations) of western Cape Cod.

## 3.3 Hydrogeology

The geology and hydrology of western Cape Cod define the hydrogeologic characteristics of the aquifer. General information on the geology and hydrology of Cape Cod can be found in the works by Oldale (1982), Guswa and LeBlanc (1985), LeBlanc et

20

al. (1986), and Oldale and Barlow (1987). This section summarizes the data on the major aquifer properties measured throughout the area. Variability of these values may be due not only to natural heterogeneity of the sediments, but also to differences in measuring techniques and data analysis (E.C. Jordan, 1989a).

### 3.3.1 Hydraulic Conductivity

Throughout the western Cape, there appears to be a general trend of decreasing conductivity from north to south and from the surface to the bedrock. The conductivity of the western Cape has been studied extensively. Geologic variability within the outwash suggests that some variability in hydraulic conductivity is likely. Nonetheless, the maximum and minimum values reported are probably biased by the analytical method or exhibit a small-scale geologic heterogeneity. An value of 380 ft/d (obtained from the Ashumet Valley pump tests and corroborated by the tracer test south of the MMR) has been accepted as a representative value of the average hydraulic conductivity of the MPP outwash sands (E.C. Jordan, 1989a).

### 3.3.2 Anisotropy Ratio

The anisotropy ratio (ratio of horizontal to vertical hydraulic conductivities, $K_h/K_v$) has been studied along with some of the hydraulic conductivity tests. Typical anisotropy values range from 10:1 to 3:1.

### 3.3.3 Porosity

Measured values of porosity range from 0.20 to 0.42. Effective porosity of the outwash is estimated from a tracer test (Garabedian et al., 1988; LeBlanc et al., 1991) to be about 0.39.

21

### 3.3.4 Hydraulic Gradient

The hydraulic gradient will be affected by the variations in water table elevations. These typically fluctuate about three feet because of seasonal variations in precipitation and recharge. During the period of a tracer test (22 months), the hydraulic gradient in the study area (Ashumet Valley) varied in magnitude from 0.0014 to 0.0020. Vertical hydraulic gradients measured during this test were negligible except near the ponds (LeBlanc et al., 1991).

### 3.3.5 Chemistry of the Water

The chemistry of the water is important to both the remediation schemes and to the sorptive uptake. Extrapolation of laboratory results to the field requires the careful examination of in situ conditions. Some of the groundwater properties (Table 3-1) may effect the sorption of contaminants. Increased salinity may, for example, "salt out" the contaminants and increase their uptake by the solid. Changes in pH may affect the distribution of the neutral species (the component taken up by the organic matter on the solid matrices) for organic acids and bases. Intuitively, temperature effects on the uptake of a solute are predicted to mirror temperature effects on its solubility. Thus, in general, a decrease in temperature will increase the sorptive uptake of a compound. All of these are discussed in greater detail in Section 5.1.4.

Table 3-1. Groundwater properties

| Property | Value |
|---|---|
| Dissolved oxygen (mg/L) | 5.0-10.0[a] |
| pH | 5-7[a] |
| Temperature | 13° C[b] |
| Salinity | ~10 mg/L[c] |

[a] E.C. Jordan (1990)
[b] LeBlanc et al. (1991)
[c] ABB Environmental Services Inc. (1992c)

# 4. Equilibrium Sorption

Sorption of contaminants by aquifer solid matrices significantly affects their fate. The effects of sorption can be felt under both natural and engineered conditions. Under natural flow conditions, sorption can reduce the bioavailability of contaminants, reduce their advected velocity and increase their longitudinal macrodispersive behavior. The sorbed species itself is capable of contaminating the aquifer for extended periods of time. In engineered conditions, (i.e. remediation schemes such as pump and treat and *in situ* bioremediation), it is useful to quantify these effects. Bioremediation schemes may be impacted by the reduced bioavailability alluded to above. Pump and treat times are prolonged because of the continuous feeding of contaminants to the aquifer from the sorbed species. Thus, the measurement of the sorptive capacity of an aquifer must be an integral part of the site characterization process.

Equilibrium sorption is studied in both lab experiments and field tests. This study dealt with the equilibrium sorption of two polycyclic aromatic hydrocarbons (PAHs) as surrogate compounds in the assessment of the behavior of three chlorinated solvents. The time course of uptake (i.e. kinetics of sorption) was monitored to indicate the time required to reach equilibrium in the laboratory experiments. The use of phenanthrene and pyrene was based on the ease of handling and measurement of these compounds in the laboratory. It was assumed that the sorption of these compounds was a partitioning process into natural organic matter and equilibrium distribution coefficients were calculated theoretically. These calculated values were then compared to experimental results to validate the use of theoretical relationships in extracting distribution coefficients for the chlorinated compounds. The distribution coefficients were then converted to parameters used in the estimation of contaminant fate and transport in the aquifer.

## 4.1 Background and Theory

Hydrophobic sorption is a partitioning process governed by a phase partitioning coefficient $K_p$ or $K_d$ (Chiou et al., 1979; Karickhoff et al., 1979, Means et al., 1980; Schwarzenbach and Westall, 1981). Distribution coefficients are used to quantify the amount of sorbed species as a function of aqueous concentration. Simply,

$$K_d = \frac{C_s}{C_w} \qquad (5.1)$$

where $C_s$ is moles of solute per kilogram of solid and $C_w$ is moles of solute per liter of solution. Thus, $K_d$ has the units of liters per kilogram. This is a linear equation which is indicative of an absorptive process.

Theoretically, at equilibrium, there are two factors that dictate the sorption of a hydrophobic solute; these are the fraction of organic matter of the solid, $f_{om}$ ($kg_{om}/kg_{solid}$), and the organic matter-water partitioning behavior of the solute, $K_{om}$ ($L/kg_{om}$). Distribution coefficients are calculated using the following equation,

$$K_d' = K_{om} \cdot f_{om} \qquad (5.2)$$

where the prime notation is used to indicate a theoretical $K_d$ value. To use the above equation, here the $f_{om}$ is approximated as twice the fraction of organic carbon, $f_{oc}$ (Schwarzenbach et al., 1993; Gu et al., 1994), a laboratory measured value.

24

### 4.1.1 Organic Matter-Water Partition Coefficient

The $K_{om}$ can be predicted from related chemical properties such as the liquid chemical aqueous solubility or the octanol-water partition coefficient, $K_{ow}$ ($L_{water}/L_{octanol}$). Many linear free energy relationships (LFER's) exist that allow the calculation of $K_{om}$ for specific solutes. The LFER used to predict $K_d$'s for phenanthrene and pyrene is given by (Karickhoff, 1981),

$$\log K_{om} = 1.01 \cdot \log K_{ow} - 0.72 \tag{5.3}$$

This LFER is used because aromatic hydrocarbons were utilized in its development. The corresponding LFER used for the prediction of the $K_d$'s for dichloroethene (DCE), trichloroethene (TCE), and tetrachloroethene (PCE) is (Karickhoff, 1981),

$$\log K_{om} = 0.88 \cdot \log K_{ow} - 0.27 \tag{5.4}$$

The predicted $K_{om}$ and the $K_{ow}$ for the compounds of interest are listed in Table 4-1.

Table 4-1. Theoretical log $K_{om}$ values calculated from log $K_{ow}$'s and equations 5.3 and 5.4.

| Compound | log $K_{ow}$ | log $K_{om}$ |
|---|---|---|
| Phenanthrene | 4.57[a] | 3.90 |
| Pyrene | 5.13[a] | 4.46 |
| c-1,2-DCE | 1.86[b] | 1.37 |
| t-1,2-DCE | 2.09[b] | 1.57 |
| TCE | 2.42[a] | 1.86 |
| PCE | 2.88[a] | 2.26 |

[a]Schwarzenbach et al. (1993).
[b]Hansch et al. (1995)

25

The variability in sorptive uptake among DCE, TCE, and PCE is much larger than the variation between c-DCE and t-DCE. In addition to this, the data for DCE are all reported as total DCE without a distinction between the two isomers (ABB Environmental Services, Inc., 1992a). In this study, an average log $K_{om}$ of 1.98 is used to assess the behavior of the total DCE in the aquifer.

## 4.1.2 Fraction Organic Matter and Fraction Organic Carbon ($f_{om}$ and $f_{oc}$)

The $f_{om}$ is the fraction of the sediment, by weight, that is composed of natural organic matter (NOM). A discussion of the nature and origin of the NOM is warranted. NOM in the environment is usually negatively charged because of the presence of carboxyl groups (Barber et al., 1992; Schwarzenbach et al., 1993). Barber et al. (1992) present a good discussion of how the sands at Cape Cod are coated with NOM. These investigators separate the sands into magnetic and non-magnetic fractions. The predominant mineral in the non-magnetic sand fraction is quartz (~50%). The pH of zero point charge (ZPC) for quartz is 2 (Parks, 1965). This means that under natural conditions at Cape Cod (pH ~ 5-7) the surface of these minerals is negatively charged. Iron oxides (e.g., positively charged FeOOH) can attach to these surfaces via electrostatic forces. This attachment results in the exposure of positive surfaces to the solution. The negatively charged NOM can now "cling onto" these surfaces via either surface complexation (Jardine et al. 1989) or ligand exchange reactions (Gu et al., 1994). In the magnetic fraction of the sands, goethite (FeOOH) is one of the predominant minerals (~20%). The pH of ZPC for geothite is 8 (Parks, 1965); the surface of the geothite is, thus, mostly positively charged. Owing to the large surface areas (small particle sizes) in these minerals, most of the NOM will be associated with this small-sized, positively charged fraction. The results presented by Barber et al. (1992) support this by suggesting that this magnetic fraction has fifty times more surface area and five times more NOM than the non-magnetic fraction.

The mechanism of NOM attachment was not investigated in this study. The NOM was quantified for two main reasons. First, theoretical distribution coefficients were calculated using the $f_{om}$ values. Second, the $f_{om}$ values were used to calculate $K_{om}$ values from the batch tests and to compare them with the theoretical $K_{om}$ values.

# 5. Experimental Distribution Coefficients

## 5.1 Laboratory Methodology

Distribution coefficients were obtained experimentally in batch tests. Batch tests provide an energetic environment in which the solute partitions into the solid matrix. Kinetic limitations (i.e., diffusion through film of water around solid aggregate, etc.) are reduced in this energetic environment. The batch methodology was used to ensure the attainment of equilibrium over a reasonable amount of time. The attainment of equilibrium was assessed by measuring the time-dependence of the aqueous solute concentration in kinetics samples. The term "kinetics samples" is used to distinguish the set of samples used to monitor the approach to equilibrium from the "long incubation" samples used to determine $K_d$. This latter set will hereon be termed "samples". The samples were stored and treated exactly the same as the kinetics samples to ensure procedural consistency. After equilibrium conditions were verified, the samples were opened and the aqueous solute concentrations were measured by synchronously scanned fluorescence spectroscopy (Vo-Dinh, 1981).

### 5.1.1 Determination of $f_{oc}$

The $f_{oc}$s of the sand samples were determined using a Perkin-Elmer 2400 CHN analyzer. The mineral composition of the Cape Cod sands was assumed to not include carbonates (Barber, 1992); pretreatment was not required to remove any inorganic carbon species. The total organic carbon (by weight) was thus taken as the fraction of the sediments that was composed of carbon. These numbers were doubled to convert the organic carbon numbers to organic matter numbers, $f_{om}$s.

The analyzer was purged with helium and oxygen to remove residue from previous runs. Then, a series of blanks and standards were run as conditioners. The standards consisted

of acetanilide weighing 1.5-2.0 mg. Three standards were run in series to check reproducibility of the samples. Before the actual sands were used, an acetanilide sample was run as an unknown sample and the values obtained for carbon, hydrogen and nitrogen were checked for accuracy (these values were known for acetanilide and should have fallen within a prescribed range). This process was continued until the blanks and the calibration numbers were acceptable. Samples were then run, interspersed with blanks and unknown acetanilide standards to ensure calibration. The sequence followed was seven to ten samples, a blank, a standard, more samples and so forth.

### 5.1.2 Batch Vials Setup

Each batch vial was set up so that approximately fifty percent of the solute was associated with the solid phase. The handling of this constraint was somewhat complex since each vial contained a mixture of phenanthrene and pyrene. The vials were optimized for phenanthrene because the fluorescence technique used distinguished small variations in the pyrene concentration better than it did for phenanthrene. To obtain a fifty percent sorbed configuration, the theoretical $K_d'$ values (Table 5-3) were used to calculate the appropriate solid-to-water ratio, $r_{sw}$. The fraction of the solute in the water at equilibrium is given by (Schwarzenbach et al., 1993),

$$f_w = \frac{1}{1 + r_{sw}K_d'}$$ (5.5)

Setting the $f_w$ equal to 0.5, the $r_{sw}$ for each sand sample (each depth) is determined from equation 5.5 (Table 5-1).

Table 5-1. Calculated experimental solid-to-water ratios ($r_{sw}$) optimized for phenanthrene. The mass of solid added to each vial is determined.

| Sample ID (depth) | $K_d$' (L/mg) | $r_{sw}$ (g solid/ml solution) | Mass of Solid in each 15 ml vial (g) |
|---|---|---|---|
| S315-5 | 6.88 | 0.15 | 2.0 |
| S315-13 | 1.56 | 0.64 | 7.2 |
| S315-2 | 0.92 | 1.09 | 10.3 |
| S315-14 | 0.76 | 1.32 | 11.5 |
| S315-9 | 1.21 | 0.83 | 8.6 |

The required mass of sand was added to each vial first. Then, the vials were filled with an aqueous solution containing HgCl (10 mg/L) to inhibit microbial growth. It was determined experimentally that this added HgCl did not significantly affect the fluorescence spectra by taking fluorescence measurements of the electrolyte solution with HgCl (10 mg/L) only. Each vial was then spiked with a certain volume (ranging from 5 μl to 30 μl) of the phenanthrene and pyrene stock. This stock was made in a methanol:methylene chloride solution (90% methanol, 10% methylene chloride). Since phenanthrene and pyrene were added simultaneously to the same vial, traditional fluorescence spectroscopy could not be used to determine aqueous concentrations. Phenanthrene and pyrene exhibit emission spectra that overlap. Potential interference between the two spectra could have resulted in erroneous data interpretations. A synchronous scanning technique was used that distinguished between the two compounds.

Two sets of batch vials (duplicates) were set up for each sand depth. Each set contained seven vials. The first was a negative control used to quantify the background fluorescence of any NOM or other fluorophores resident in the solids and entrained from the energetic mixing conditions. The six remaining vials were spiked with different volumes of the stock solution yielding aqueous concentrations of pyrene from 8% to 70% of its solubility, depending on the sand used. The dependence on the sand used occurred

because of the above calculated solid-to-water ratios. As this ratio increases, the amount of solid in the vials increases, effectively decreasing the volume of water in the vials. Since an equal volume of the stock was added to each respective vial, the vials with the lower water volumes had higher effective concentrations. For the phenanthrene samples concentrations ranged from 9% to 60% of this compounds solubility. This procedure was repeated for each sand depth. A linear regression through the six points in each set was used to determine the $K_d$. With appropriate regression plotting units (moles/kg of solid vs. moles/L of water), the $K_d$ was determined as the slope of this line. In addition to these vials, two positive control vials were set up. These vials contained water and the mixture of phenanthrene and pyrene only and were used to monitor the amount of solute uptake by the vessel (glass and Teflon sorption) as well as to detect other losses from the system (volatilization, photodegradation, etc.).

The kinetics runs consisted of 14 batch vials. Each vial contained S315-13 (58-60' depth) sand and was spiked with 25 µl of the stock solution; an effective vial concentration of 43% of solubility for phenanthrene and 50% of solubility for pyrene was obtained. This sand was used because of its abundance. A spike volume of 25 µl was used for convenience.

The samples and the kinetics samples were prepared at the same time to ensure compatibility and homogeneity in the samples. All of the vials were then placed in a tumbler and rotated at a rate of 15 complete rotations per minute for an hour each day. Once the kinetics results showed the attainment of equilibrium (see Figures 5.4 and 5.5, for example), all of the samples were removed and the aqueous concentrations of phenanthrene and pyrene were measured. The sorbed concentration was the concentration in the aqueous phase subtracted from the total concentration in the vial. The total concentration in the vial is equal to the concentration of the spike adjusted for any losses to the Teflon lining the screw cap. This loss was quantified by calculating the loss of the compounds in the control vials (i.e., vials with water and solutes only). These corrections were small and resulted in adjustments of $K_d$ of ≤ 5%. The concentration of

the spike was calculated using standard curves that encompass 10 to 40% of the solubility of phenanthrene and 5 to 45% of that of pyrene (Figure 5.2).

### 5.1.3 Synchronous Scanning and the Performance of the Standard Curves

Synchronous scanning was used to simultaneously measure the abundance of pyrene and phenanthrene dissolved in the vials. In this methodology, both the emission and excitation spectra were scanned simultaneously with a fixed wavelength offset between the two, $\Delta\lambda$ (Vo-Dinh, 1981). By using this technique, a unique peak was obtained for each compound in the solution. At first, a $\Delta\lambda$ equal to 45 nm was chosen. This offset provided two distinct peaks, one for each of the compounds; the peak for phenanthrene was at 297 nm and that for pyrene was at 332 nm (Figure 5.1b). The background fluorescence from the NOM and other fluorophores showed a significant signal between wavelengths of 280 and 300 nm. This signal was large enough to interfere with the phenanthrene signal. Thus, a $\Delta\lambda$ equal to 55 nm was used in this study. The only drawback of using this setting is that at a wavelength of 315 nm, a peak which is approximately 80% of the pyrene peak appears (Figure 5.1a). The "hump" occurring at ~320 nm (Figure 5.1a) is of some concern since it could be an artifact of the procedure. Ideally, peaks corresponding to compounds should be distinct and interference between them should be reduced. Although the $\Delta\lambda$ = 45 nm provided more distinct spectra, the $\Delta\lambda$ = 55 nm setting was used for convenience.
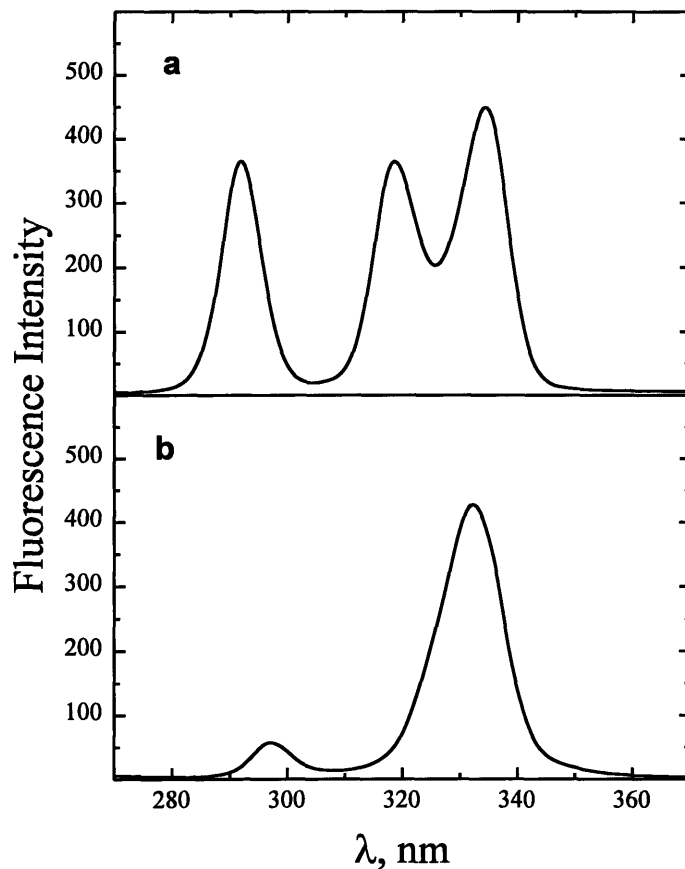
Figure 5-1. Synchronously scanned fluorescence spectra for sample +CTA (positive control). In Figure a, $\Delta\lambda = 55$ nm and in Figure b, $\Delta\lambda = 45$ nm. Other settings : Slit widths of emission and excitation beams were set at 7 nm, scan speed was set at 1500, the increment was set at 0 nm (used for three dimensional spectra), and spectra were scanned from 270 nm to 370 nm.

One way to ensure that this approach (using $\Delta\lambda = 55$nm) was acceptable was to use standard solutions to calibrate the fluorescence measurements. As can be seen in Figure 5.2, both the $\Delta\lambda = 45$ nm and $\Delta\lambda = 55$ nm produced linear standard curves. From Figure 5.2, it is apparent that both settings produced precise results. With each incremental increase in concentration, the spectral intensity of the solution increased. From these results, the use of the $\Delta\lambda = 55$ nm setting was justified.

33
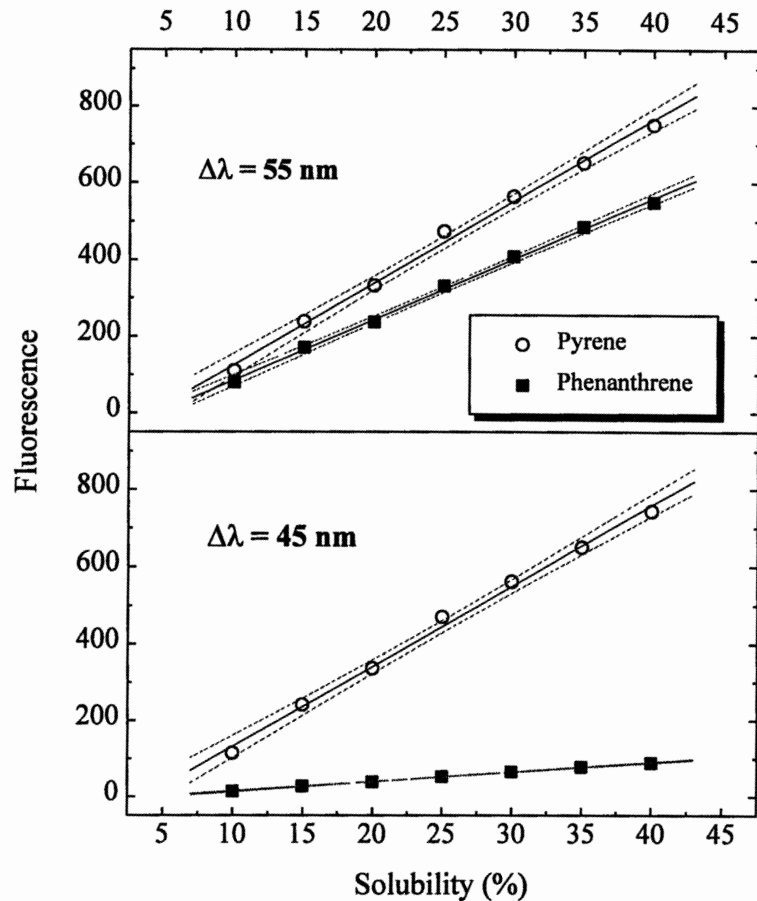
Figure 5-2. Standard curves for pyrene and phenanthrene at two different wavelength offset ($\Delta\lambda$) settings. For $\Delta\lambda = 55$ nm, the pyrene regression was Fluorescence Intensity (FI) = 21.3($\pm$0.64)·Solubility(S) - 86.6($\pm$17.3) ($r^2 = 0.995$) and the phenanthrene regression was FI = 15.8($\pm$0.32)·S - 71.9($\pm$8.5) ($r^2 = 0.998$). For $\Delta\lambda = 45$ nm, the pyrene regression was FI = 20.9($\pm$0.63)·S - 77.1($\pm$16.8) ($r^2 = 0.996$) and the phenanthrene regression was FI = 2.5($\pm$0.04)·S - 11.3($\pm$0.97) ($r^2 = 0.999$). The dotted lines represent 95% confidence intervals.

` was evident that synchronous scanning provided an effective means of identifying and q ntifying the amount of each of the dissolved species in the aqueous phase. Syι hronous scanning had other advantages as well. For the concentrations and comp nds used in this study, dilution was not required. The traditional fluorescence spectro opy methodology would have required the dilution of most of the samples.

Dilution of and repeated handling of samples could result in erroneous results. It was desirable to reduce all factors that could have introduced error in the analyses. Synchronous scanning provided enough resolution and sensitivity to allow for direct withdrawal and re-injection of the supernatant from and to the sample vials. This was important because in the traditional fluorescence spectroscopic methodology, the diluted sample could not be returned to the vials. Thus, each time a kinetics vial was opened and the fluorescence of the supernatant was measured, a larger headspace of air was developed. This headspace could have resulted in erroneous data interpretations especially when the kinetics samples are monitored over long periods of time. This effect and methods for reducing it have been discussed by Ball and Roberts (1991).

Using synchronous scanning, fluorescence measurements were taken for each sample. The fluorescence intensity needed to be corrected for an inner filter effect (Vo-Dinh, 1981; Gauthier et al., 1986). Simply stated, the inner filter effect quantifies a "loss" of energy in the system. Absorbance of aqueous species caused the dissolved species at the end of the cuvette to not "experience" the same excitation as those at the front of the cuvette (relative to the incoming beam intensity). These effects were corrected for by absorbance measurements taken with a spectrophotometer. The expression used for the correction of the fluorescence measurements is given by Gauthier et al. (1986). In addition to correcting for the wavelengths used in generating the synchronous spectra, an additional absorbance reading was taken at 700 nm. At this wavelength, the decrease in light through the sample was attributed to scattering by particles. This measurement was taken to be able to distinguish solute absorption from particle scattering. A difference between the absorption and scattering gave the true absorption value. Scattering absorbance values were insignificant in most of the samples.

### 5.1.4 Laboratory Procedures and Environments Affecting Sorption

Laboratory experiments were conducted under controlled conditions. In the field, there are many factors that change. The background concentration of electrolytes and

contaminants and temperature changes can affect solute fate. In the lab, the stock solution of pyrene and phenanthrene was made in a methanol:methylene chloride mixture. The effects of cosolvents may have to be considered because in field, solute concentrations are small enough that species act as cosolutes and not cosolvents.

*Effect of Electrolyte Solution Composition on Sorption*

The salinity of the water can effect the sorptive uptake of solutes. Schwarzenbach et al. (1993) present an expression that allows the adjustment of $K_{om}$'s of solutes for the presence of dissolved salts. Assuming that the salinity of the aquifer was equal to the sodium chloride concentration (10 mg/L, ~0.0002M) (ABB Environmental Services Inc., 1992c) and using the expression given by Schwarzenbach et al. (1993), the difference between the $K_{om}$ in "saline" water and that in "fresh" water was less than 0.00006 log units (0.01%), absolutely negligible.

*Effect of Temperature on Sorption*

In a recent paper (Piatt et al., 1996), the effect of temperature on the sorption of naphthalene, phenanthrene, and pyrene on sediments similar to those used here ($f_{oc}$ = 0.02%) is discussed. These investigators found that a temperature change of 22° (from 26°C to 4°C) increased the $K_d$'s by a factor of 1.1 to 1.6. Also, the desorption rate constants decreased 1.2 to 2.6 times with the same temperature change. These results indicate that the laboratory determined $K_d$ values might not be representative of those in groundwater bodies. For aged contaminants, the desorption rates may be significantly affected by this temperature change. In the Cape Cod aquifer, an average temperature of 13°C is observed (LeBlanc et al., 1991) compared to the laboratory measured temperature of 23°C. For pyrene, a temperature change from 20°C to 10°C increases the $K_{om}$ by 30%

(increasing the $K_d$) (Schwarzenbach et al., 1993). These effects are small and are expected to be much smaller for the chlorinated solvents. The distribution coefficients were, thus, not adjusted for temperature changes.

*Cosolvent Effects on Sorption*

An additional effect that had to be considered is the interactions of cosolvents on the observed laboratory distribution coefficients. The concentration of methanol and methylene chloride in the vials (as cosolvents) may have been large enough to effect the distribution of the solutes. Similar to assessing the effects of salinity on $K_d$, it was assumed that $K_{om}$ was affected by cosolvents to the extent that solubility changed. An expression for the $K_{om}$ of a mixture is given by Schwarzenbach et al. (1993). The fraction of cosolvent introduced ($f_c$) in the vials ranged from approximately 0.0003 to 0.003. Here $f_c$ was assumed to be 0.003 to measure the largest enhancement of solubility (lowering of $K_{om}$ and $K_d$). The $K_{om,mix}$ values were calculated to be lower than the corresponding $K_{om}$ values by a factor of 0.04. Thus, the introduction of cosolvents had a minimal effect on the uptake of the solutes.

## 5.2  Laboratory Results

### 5.2.1  Laboratory Determined $f_{oc}$

The samples used in this study were obtained from the USGS.  The sampling location was located in close proximity to the CS-4 plume (Figure 5-3).
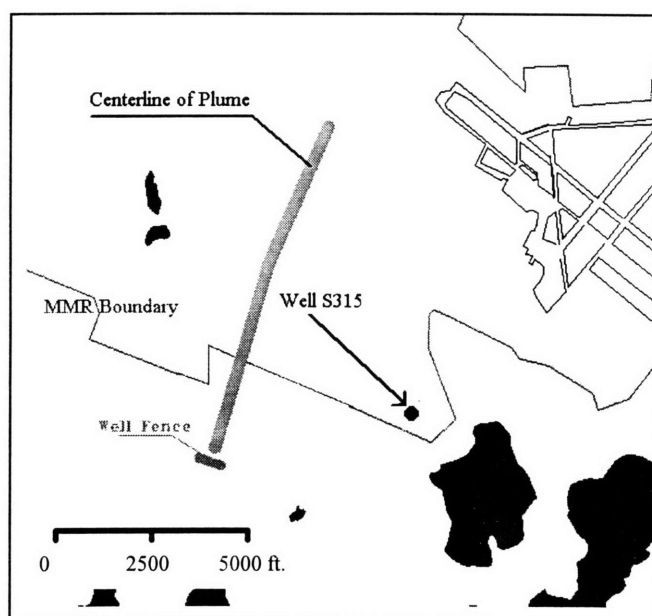


Figure 5-3.  Location of Well S315 relative to the centerline of the CS-4 plume.

The fraction of organic carbon of the sands used in this study are fairly low (generally less than 0.01%) (Table 5-2).  Schwarzenbach and Westall (1981) suggest that when the $f_{oc}$ is less than 0.1% ($f_{om} < 0.2\%$), adsorption to the mineral surfaces becomes important in the distribution of the nonionic solute.  However, as a first assumption, organic phase partitioning was taken as the only source of solute uptake.

Table 5-2. Sand Identification including measured $f_{oc}$s and hydraulic conductivities.

| Sand ID | Sand Depth (feet) | $f_{oc}$ ($\pm\sigma$), (%) | K, cm/s[a] |
|---------|-------------------|----------------------------|------------|
| S315-5 | 18-20 | 0.0433 (0.0015) | 0.012 |
| S315-13 | 58-60 | 0.0098 (0.0005) | 0.041 |
| S315-2 | 73-75 | 0.0058 (0.0013) | 0.100 |
| S315-14 | 78-80 | 0.0048 (0.0008) | 0.060 |
| S315-9 | 88-90 | 0.0076 (0.0011) | 0.037 |

[a] The K values approximated from Figure 4.8.5 of Thompson (1994).

Table 5-2 also contains hydraulic conductivity values, $K$, obtained from Thompson (1994). These values were measured in the laboratory with saturated sand samples. A weak trend can be observed where the sediment fractions with the highest $f_{oc}$ values (e.g., S315-5, S315-13 and S315-9) have the lowest hydraulic conductivity values. This can be attributed to the presence of fine particles. Flow through these particles is harder because the hydraulic conductivity can be represented (roughly) by the square of the diameter of passage (Domenico and Schwartz, 1990). The diameter of the passage is roughly the same as the diameter of the particles of the medium. Thus, finer particles present narrower passages to the water, restricting its flow. Also, as discussed previously, finer particles have larger surface areas and can attract and retain more organic matter, resulting in higher $f_{oc}$'s.

## 5.2.2 Theoretical Distribution Coefficients

The theoretical distribution coefficients were calculated using the laboratory measured $f_{om}$ data and the calculated $K_{om}$ data. The $K_{om}$ data have been tabulated previously (Table 4-1). From the measured $f_{oc}$ data (Table 5-2) and the calculated $K_{om}$ data (Table 4-1), theoretical distribution coefficients were calculated (Table 5.3). The error values in the parentheses are the errors associated with the determination of the $f_{oc}$ (or $f_{om}$) values. The distribution coefficients vary (with depth) by a factor of 10 (Table 5.3). . If phase partitioning is assumed to dominate the sorption of these compounds, in order to understand the influence of sorption on plume transport it is important to determine the

location and dimensions of the plume so that a correct assessment of sorption effects can be made.

Table 5-3. $K_d'$ values calculated from the linear equilibrium sorption equation $K_d'=K_{om}f_{om}$. The values in parentheses represent the error in the calculated values due to the error in the $f_{om}$ measurements.

| | | $K_d'$ (L/kg), (±error) | |
|---|---|---|---|
| Sample ID | $f_{om}$, % (±error) | Phenanthrene | Pyrene |
| S315-5 | 0.087(0.0030) | 6.8(0.24) | 25(0.87) |
| S315-13 | 0.020(0.0010) | 1.6 (0.079) | 5.7 (0.29) |
| S315-2 | 0.012(0.0026) | 0.92 (0.21) | 3.3 (0.75) |
| S315-14 | 0.0096(0.0017) | 0.76 (0.13) | 2.8(0.48) |
| S315-9 | 0.015(0.0022) | 1.2(0.17) | 4.4 (0.63) |

## 5.2.3 Kinetics Runs

The attainment of equilibrium of the samples was monitored through the use of kinetics samples. The kinetics samples were set up at the same time and according to the same procedure as the samples. Due to time constraints, the samples were opened and measured after a 10 day equilibration time. The fluorescence of the kinetics samples were, however, measured for 40 days to ensure the attainment of equilibrium. After the 10 day period, the samples had reached equilibrium (Figure 5.4). This is because
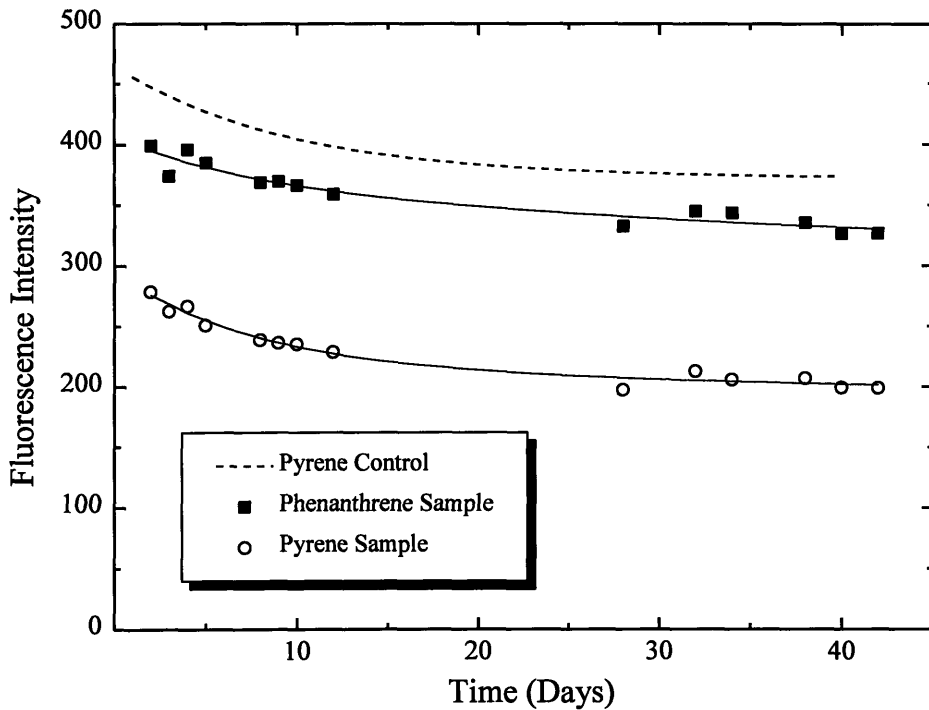
Figure 5-4. The time-series of uptake for sample K2. Apparently, complete equilibrium has not been reached after 40 days. However, control samples (water and solute only, dashed line) show similar behavior indicating another loss mechanism besides sorption (i.e., loss to Teflon).

duplicate control vials (water and phenanthrene and pyrene only) showed similar trends (Figure 5-4, dashed line). This trend was attributed to loss to the Teflon lining the screw cap.

The equilibration time of 10 days used in this study is supported by previous studies. Ball and Roberts (1991) studied the sorption of halogenated organic chemicals and found equilibration times ranging from 0.01 day to over 100 days. These investigators attributed this decline in concentration mainly to slow sorption kinetics. Similar results were given by Holmén (1995) who found equilibration times ranging from 24 minutes to two days.

Other reasons for the observed reduction in concentrations were possible. For example, each time a measurement was taken, the sample was subjected to light ranging from 270 nm to 370 nm twice (once by the fluorometer and once by the spectrophotometer). The electronic absorption spectra of phenanthrene (in hexane) spans a wavelength range from 200 nm to 350 nm (Schwarzenbach et al., 1993). This means that phenanthrene is capable of absorbing light in this range. When phenanthrene was promoted to an excited state, it could have undergone photochemical reactions (Schwarzenbach et al., 1993). It is conceivable that each exposure to the incident light caused a decline in the phenanthrene concentration.

The same loss mechanisms were observed in the control vials as well. By normalizing the kinetics sample fluorescence to that of the control vials, a relative loss rate was observed. The only extra loss mechanism in the normalized system should have been sorption. Figure 5-5 represents a plot of the normalized concentrations of phenanthrene and pyrene for the K2 kinetics sample. The slopes of the lines were indistniguishable from zero indicating that the loss mechanisms in the kinetics samples and the control samples were essentially the same.
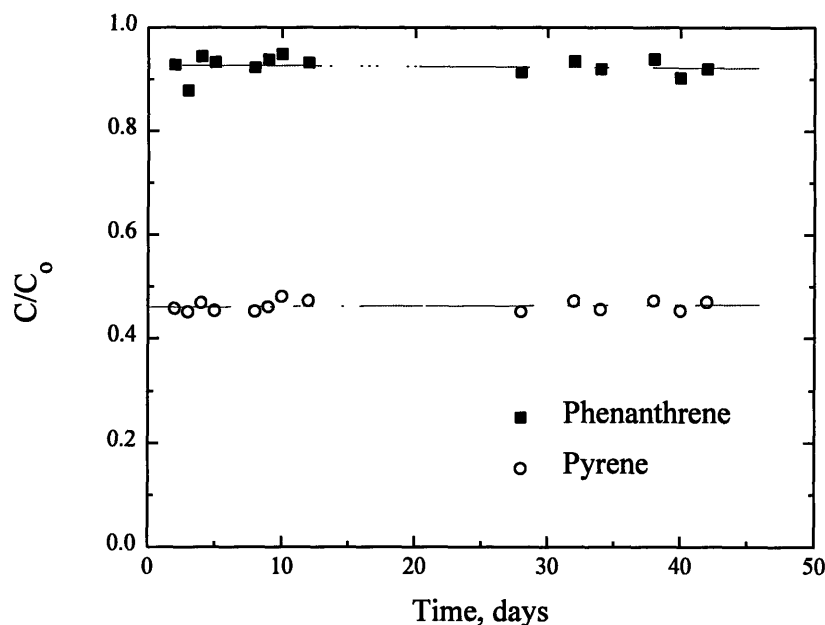
Figure 5-5. Control normalized kinetics sample concentrations (K2). The flat slope indicates the attainment of equilibrium. Slope and intercept of the phenanthrene regression were -0.00015 (± 0.0019) and 0.93 (± 0.008), respectively. The slope and intercept of pyrene were -0.0027 (± 0.0031) and 0.46 (± 0.004), respectively.

To ensure that the slope was zero, other plots were analyzed (samples K2-K7) and an aggregate slope was calculated (Table 5-4). The standard deviations of the regressions were larger than the average slopes (Table 5-4). This indicates that the slopes were indistinguishable from zero indicating and that equilibrium conditions were reached.

Table 5-4. The slope and intercept of the normalized plots of concentrations for the kinetics run. The concentration are normalized to control vials.

| Compound | Slope | Std. Deviation |
|---|---|---|
| Phenanthrene | -0.000062 | 0.0063 |
| Pyrene | -0.000029 | 0.0076 |

Given all the complexities of the identification of the system losses, and due to the fact that the error in the slope regressions were larger than the slopes, the ten day period was chosen as the representative equilibration time.

## 5.2.4 Equilibrium Distribution Coefficients, $K_d$s

For each system, the calculated sorbed concentration was plotted against the measured aqueous concentration (Figure 5-6). The slopes of Figure 5-6 were the $K_d$ values of each particular systems.
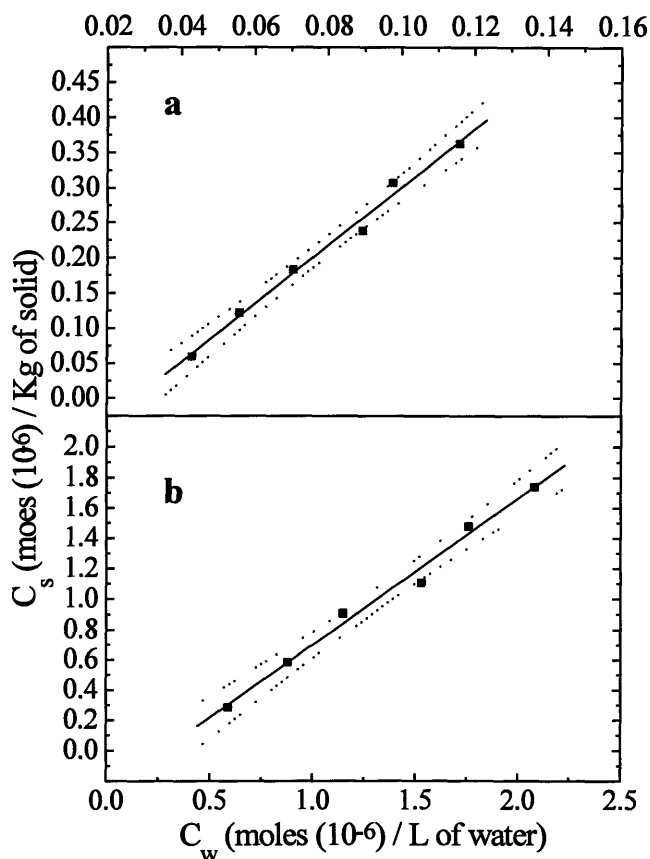


Figure 5-6. The equilibrium distribution of pyrene (Figure a) and phenanthrene (Figure b) for the 73-75 foot depth (Sample S315-2). The slopes of the regressions were the respective $K_d$ values. For pyrene a slope of 4.1 was obtained ($r^2 = 0.99$). For phenanthrene a slope of 0.96 was obtained ($r^2 = 0.99$). The dotted lines represent 95% confidence intervals.

Each $K_d$ obtained for each depth was an average of duplicate samples (Table 5-5). Figure 5-6 illustrates the $K_d$ obtained from two of the samples. At each depth, two of these figures were generated and the depth representative $K_d$ was taken as the average of the individual $K_d$'s. The error was a composite of the individual errors obtained from the linear regression analyses.

Table 5-5. Experimentally determined $K_d$ values. [a]

| Sample | Phenanthrene $K_d$, L/kg (±error) | Pyrene $K_d$, L/kg (±error) |
|---|---|---|
| S315-5 | 6.3 (1.0) | 30 (5.0) |
| S315-13 | 1.7 (0.31) | 7.3 (1.2) |
| S315-2 | 1.1 (0.23) | 4.4 (0.92) |
| S315-14 | 0.99 (0.23) | 4.3 (0.75) |
| S315-9 | 0.95 (0.13) | 3.7 (1.1) |

[a] Values are averages of duplicates for each sample

It is important to see how these experimental values compare with the theoretically calculated values ($K_d'$). It is assumed that if the pyrene and phenanthrene $K_d$ values are appropriate, then the $K_d'$ values of DCE, TCE, and PCE are usable in assessing contaminant availability and transport.
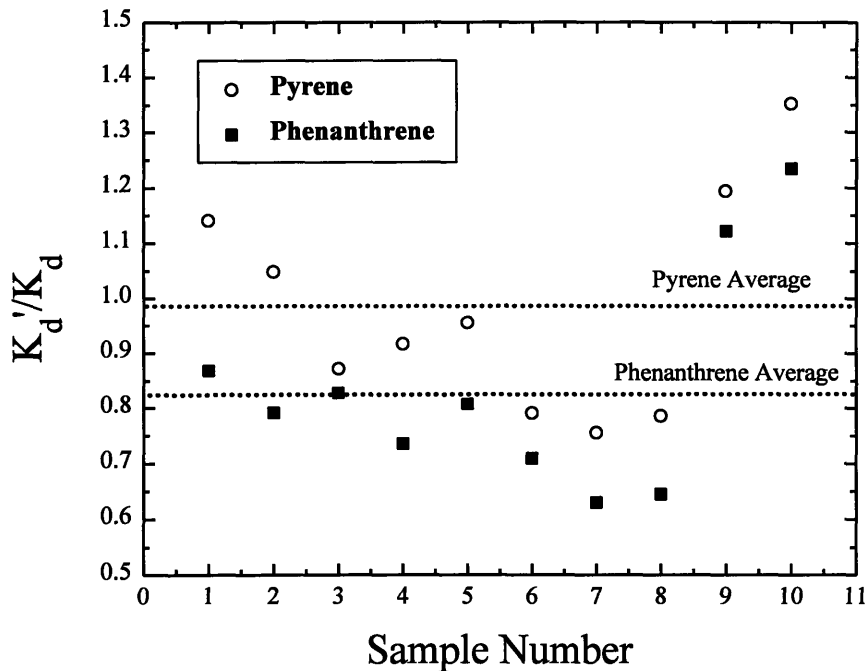
Figure 5-7. The ratio of $K_d'$ to $K_d$. The horizontal lines represent the average ratio between $K_d'$ and $K_d$. The intercept was 0.84 (±0.20) for pyrene and 0.98 (±0.20) for phenanthrene. Given the errors, the intercepts are indistinguishable from zero. Thus, $K_d'$ is taken to be representative of $K_d$.

The theoretical distribution coefficients are consistent with the experimentally derived distribution coefficients (Figure 5-7). The horizontal lines represent the average ratios between the theoretical and experimental $K_d$ values for phenanthrene and pyrene. The average ratio for pyrene is 0.84 with an error of ±0.20. The average ratio for phenanthrene was 0.98 with an error of ±0.20. In both cases. the averages are indistinguishable from zero indicating that the theoretical values are in good agreement with the experimentally derived values. Based on these findings, the $K_d'$ values for DCE, TCE, and PCE were calculated using equation 5.2 (Table 5-6)

Table 5-6. Theoretical $K_d'$ values for DCE, TCE, and PCE.

| Sample ID | $f_{om}$, % ($\pm$error) | $K_d'$ (L/kg), ($\pm$error) | | |
| --- | --- | --- | --- | --- |
| | | DCE | TCE | PCE |
| S315-5 | 0.087(0.0030) | 0.026 (0.00091) | 0.062 (0.0022) | 0.16 (0.0055) |
| S315-13 | 0.020(0.0010) | 0.0059 (0.0003) | 0.014 (0.00072) | 0.036 (0.0018) |
| S315-2 | 0.012(0.0026) | 0.0035 (0.00079) | 0.0084 (0.0019) | 0.021 (0.0047) |
| S315-14 | 0.0096(0.0017) | 0.0029 (0.00051) | 0.0070(0.0012) | 0.017(0.0031) |
| S315-9 | 0.015(0.0022) | 0.0046 (0.00066) | 0.011(0.0016) | 0.028(0.0040) |

Converting the $K_d$ values obtained experimentally to $K_{om}$ values is also instructive. As can be seen in Figure 5-8, all of the $K_{om}$ values for both phenanthrene and pyrene extracted from the $K_d$ data were within the range of prediction. The pyrene $K_{om}$ values were consistently, but not significantly larger than the predictive window. The reason for this was not known. However, the consistency of the data set overshadowed the departure from the predicted values. Discrepancies in the comparison of theoretical and experimental distribution coefficients have been observed previously (Holmén, 1995). Some of the reasons forwarded for this behavior were slow sorption and different site availability for the different compounds (because of size differences). These descriptions could explain some of the discrepancy seen here (Figure 5-7 and Figure 5-8).

47
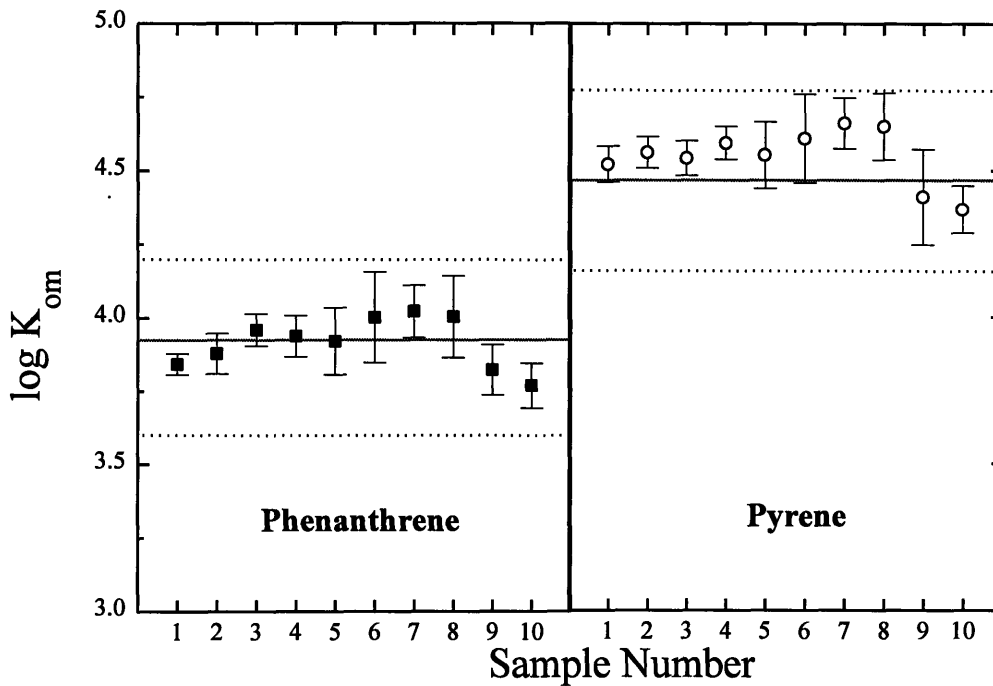
Figure 5-8. Calculated $K_{om}$ values from experimental $K_d$ values of phenanthrene and pyrene. The solid line represents the $K_{om}$ values obtained from the regression given in equation 5.3. The dotted lines represent the factor of 2 predictive interval for this regression.

## 5.3 Implications of Distribution Coefficients

The effects of these $K_d$ values on field-scale fate and transport of contaminants were assessed. First, the effects of nonequilibrium sorption were considered. Then, following this, the use and meaning of $K_d$ values are discussed.

### 5.3.1 Kinetic vs. Equilibrium Sorption

One issue in extrapolating laboratory derived results to field-scale properties is the fact that under natural gradient conditions, the solute will not have enough time to equilibrate with the solid. This would result in lower retardation values. The relative importance of

48

porewater advection vs. diffusion-controlled sorption can be inferred from a Damkohler number, $D_{klr}$, a dimensionless number. The Damkohler number is defined by,

$$D_{klr} = \frac{v}{l(k'_f + k_r)} \qquad (5.6)$$

where $v$ is the average pore velocity of the solutes, $l$ is the distance over which the processes are to be compared and $k_f$ and $k_r$ are the forward and reverse sorption rates, respectively. The characteristic correlation length scale at Cape Cod is estimated to be approximately 140 ft. This was calculated assuming a macrodispersivity of 20 m (Lázaro, 1996) and using equation 5.10 to obtain $\lambda_1$, the correlation length scale. The advection velocity was 0.24 m/d (corresponding to 0.8 ft/day, Lazaro, 1996). Since Holmén (1996) used sands similar to those used in this study (iron oxide covered sands with $f_{oc} \sim 0.06\%$), the reverse sorption rate constant used in that study was taken to be representative of the behavior of the Cape Cod sands. This assumption may be invalid since the rate constant is dependent on the sediments used and field-scale heterogeneity makes its prediction difficult. As a first assumption, however, the $k_r$ number was used to approximately quantify $D_{klr}$. Thus, $k_r$ is taken to be 2.4 day$^{-1}$. The $k'_f$ is equal to $(R-1)k_r$ (Holmén, 1995). Using an average retardation factor of 1.13 (average of the $R_{eff}$ of the three solutes, see Table 5-7), $k'_f$ is calculated to be 0.31 day$^{-1}$. Using these values, the $D_{klr}$ was calculated to be $\sim 0.001$. This implies that on a length scale comparable to the scale over which physical properties such as hydraulic conductivity, are correlated, sorption equilibrium will be reached. For this reason, it is important to quantify the sorptive capacity of the sediments in order to understand the mechanisms controlling contaminant fate.

## 5.3.2 Effects of Distribution Coefficients on Contaminant Transport

The implications of the calculated $K_d'$ of $c$-DCE, $t$-DCE, TCE, and PCE are discussed because these are the contaminants of interest. One way to analyze the effect of the partitioning of these compounds is by examining the differential equation for the three dimensional solute transport through porous media (Equation 5.8). The equation is simplified by assuming constant porosity ($n$=0.39, Garabedian et al., 1988), constant bulk density ($\rho_b$ = 1.9 kg/L, Foster-Reid, 1994) and linear sorption (i.e., $C_s = K_d C$).

$$\frac{\partial C}{\partial t} + \frac{u}{R}\frac{\partial C}{\partial x_i} = \frac{\partial}{\partial x_i}\left(\frac{D_{ij}}{R}\frac{\partial C}{\partial x_j}\right) - kC \qquad (5.8)$$

$C$ = aqueous concentration of solute (moles/L)
$D_{ij}$ = the dispersivity tensor (m$^2$/day)
$k$ = first order degradation constant (1/day)
$u$ = advection velocity (m/day)
$R$ = retardation factor

The retardation factor is a unitless number defined by,

$$R = 1 + \frac{\rho_b K_d}{n} \qquad (5.9)$$

This factor acts to reduce the advection of solutes. In using a term such as the retardation factor, local equilibrium has to be assumed (the local equilibrium assumption, LEA). This means that the time-scale of solute partitioning is taken to be much smaller than the time-scale of advective transport. Valocchi (1985) presents a good discussion on the validity and justification of this assumption. In the above kinetics runs, it was seen that the solute takes at least ten days to reach equilibrium. Also, the Damkohler number suggests that this assumption may be invalid.

Using equation (5.9) and the theoretically derived $K_d'$ values, retardation factors were calculated for the contaminants of interest (Table 5-7).

Table 5-7. Theoretical retardation values. Values in parenthesis represent error.

| Sample ID | R ($\pm error$) | | |
| | DCE | TCE | PCE |
|---|---|---|---|
| S315-5 | 1.1 (0.04) | 1.30 (0.05) | 1.77 (0.06) |
| S315-13 | 1.03 (0.05) | 1.07 (0.05) | 1.18 (0.06) |
| S315-2 | 1.02 (0.23) | 1.04 (0.23) | 1.10 (0.25) |
| S315-14 | 1.01 (0.18) | 1.03 (0.18) | 1.08 (0.19) |
| S315-9 | 1.02 (0.15) | 1.05 (0.15) | 1.14 (0.16) |

To obtain a single retardation factor that represents the aquifer horizontally, the calculated factors were arithmetically averaged over depth. This resulted in effective retardation factors, $R_{eff}$s, which are rough representations of the aquifer characteristics (Table 5-8).

Table 5-8. Effective retardation factors, $R_{eff}$.

| Compound | $R_{eff}$ |
|---|---|
| DCE | 1.04 |
| TCE | 1.10 |
| PCE | 1.25 |

Barber et al. (1988) found that the retardation factors of TCE and PCE equal to unity in an adjacent contaminant plume at Cape Cod. This value was obtained by normalizing an estimated time of travel of the solutes to the time of travel of boron, taken to be a conservative tracer. The plume studied by these investigators is located approximately 90 feet below ground surface. At this depth (Sample S315-9 in Table 5.7) similar retardation factors were obtained here (taking into account the calculated errors). It is instructive, however, to assess the possible effects of the effective retardation factors on plume fate.

51

Assuming that the validity of this data stretch over a larger extent of the aquifer, the calculated average retardation factors were used to assess plume transport behavior. According to these values, and neglecting macrodispersivity, the transport of DCE, TCE and PCE will take 4%, 10%, 25%, longer, respectively, than expected. This could have significant impacts on remediation systems. The current pump and treat system for the Cape Cod aquifer is modeled to take 70 years to remove the contaminants (Lazaro, 1996). A 25% in this pumping time results in a total pumping years of over 88 years (for PCE). These additional pumping years can become very expensive.

In the modeling and understanding of plume transport, it is imperative to account for other factors. One such factor is the amount of spreading experienced by the contaminant plume due to field-scale heterogeneity (i.e., macrodispersion). This macrodispersion is believed to dominate (in the longitudinal direction) over the hydrodynamic dispersivity if sufficient field-scale heterogeneity exists. There are many factors involved in calculating this parameter. The longitudinal macrodispersivity, $A_o$, describes the spreading in the direction of flow. Gelhar and Axness (1983) provide an expression for longitudinal macrodispersivity:

$$A_o = \frac{(\sigma_{\ln K})^2 \lambda_1}{\gamma^2} \tag{5.10}$$

where $\sigma^2_{\ln K}$ is the variance of $\ln K$ ($K$ is the hydraulic conductivity of the aquifer), $\lambda_1$ is the horizontal correlation scale and $\gamma$ is given by,

$$\gamma = \frac{q}{K_G J} \tag{5.11}$$

Here, $q$ is the specific discharge, $K_G$ is the geometric mean of the hydraulic conductivity, and $J$ is the mean hydraulic gradient. The value for the longitudinal macrodispersivity for a conservative substance at Cape Cod is estimated to be 20 m (Lazaro, 1996). However, for sorbing solutes, an adjustment to this value has to be made. Variability of sorption can produce an enhanced longitudinal dispersivity (Garabedian et al., 1988); this effect is more important when the sorption coefficient and hydraulic conductivity are negatively correlated (Figure 5-9, Figure 5-10, and Figure 5-11).
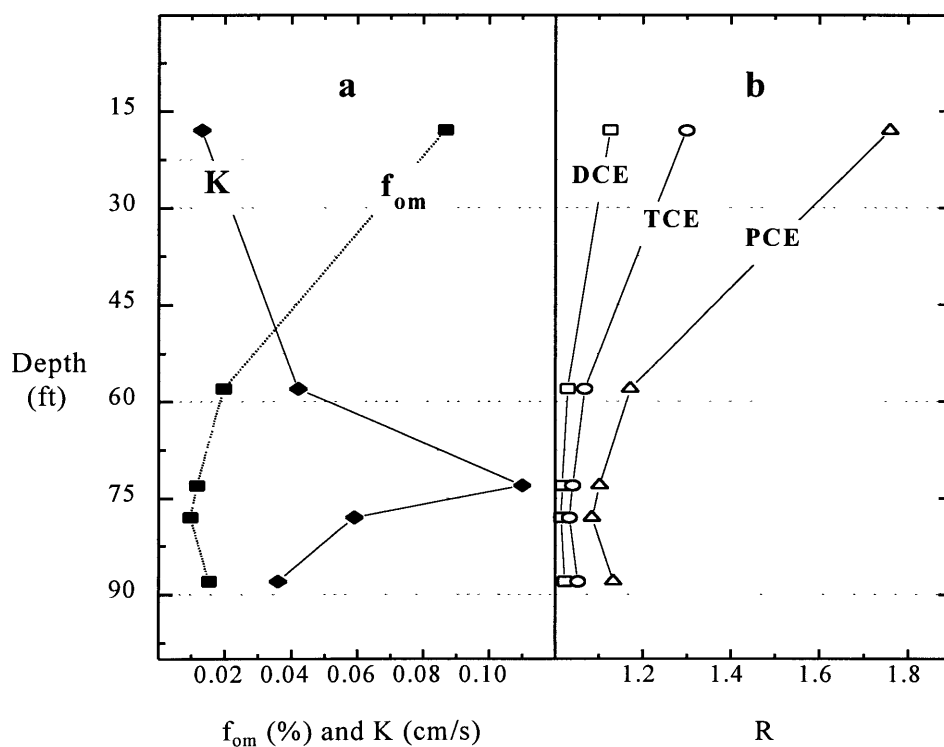


Figure 5-9. The relationship between $f_{om}$ and $K$ with depth is shown in figure a. The calculated retardation factors are shown in figure b. As expected, the $f_{om}$ is inversely related to $K$.

Fine materials may result in both reduced conductivities and higher sorptive uptake (Figure 5-9). In Figure 5-9b, the calculated retardation factors are shown and necessarily follow a similar trend to that of $f_{om}$. The large $f_{om}$ at a depth of 18 feet is paired with a

low hydraulic conductivity and high $R$ values. The retardation of the solutes causes variability in their transport velocities. This additional variability results in a larger spreading of the contaminant than quantified by $A_o$. The enhanced macrodispersivity is defined by a reactive longitudinal macrodispersivity, $A_{11}$ by (Gelhar, 1993):

$$A_{11} = A_o \left\{ \left[ 1 + \gamma \frac{\sigma_R}{\bar{R}\sigma_{\ln K}} \sqrt{\varsigma} \right]^2 + (1-\varsigma) \frac{\sigma^2_R \lambda_\eta}{\bar{R}^2 \sigma^2_{\ln K} \lambda_1} \gamma^2 \right\}$$    (5.12)

$\lambda_\eta \approx \lambda_1$, $\bar{R}$ is the mean retardation factor and $\sigma_R$ is the variance of the retardation factor. The parameter $\varsigma$ is determined from correlations of $R$ and $\ln K$ (see Figure 5-10). The other variables have been previously defined. The above expression stems from the general relationship between $R$ and $\ln K$ (Figure 5-10)
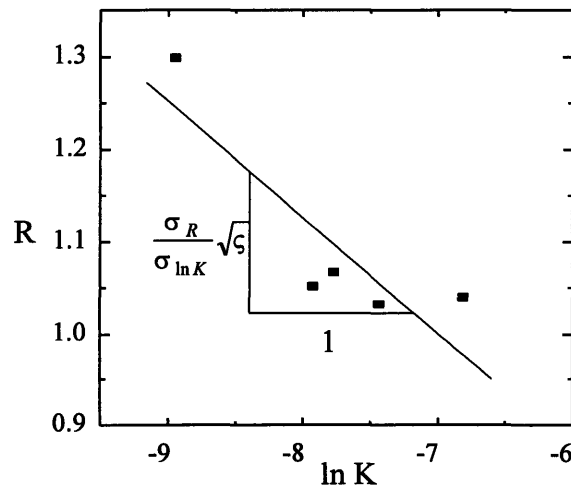


Figure 5-10. Relationship between $R$ and $\ln K$ for TCE. The slope of the line is - 0.126 which represents the quantity included in the figure.

The sands used in this study have been previously used by Foster-Reid (1994) and Thompson (1994), and $K$ values have been measured. By measuring the retardation of

the same samples, a correlation can be developed and conclusions from this correlation on plume transport can be drawn. It is important to conduct these tests on the same samples to be able to develop these correlations (Talbott and Gelhar, 1994). Figure 5.11 shows the relationship of $R$ and $ln$ $K$ for DCE, TCE and PCE. The $K$ values have been obtained from Thompson (1994) and have been included in Table 5.2. From the slope of these figures, $\zeta$ can be determined which represents the fraction of $\sigma^2_R/\bar{R}$ that is correlated with $ln$ $K$ (Talbott and Gelhar, 1994).
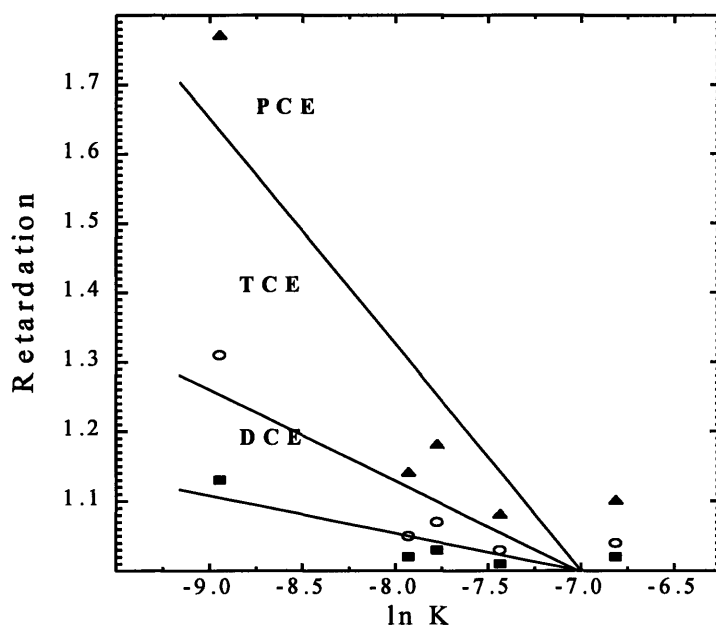


Figure 5-11. Relationship between $R$ and $ln$ $K$ for the three compounds of interest. The slopes for DCE, TCE, and PCE are -0.05, -0.13, and -0.33 respectively. The $r^2$ values for the DCE, TCE, and PCE plots are 0.720, 0.750, and 0.764 respectively.

The retardation factors of each of the solutes were correlated inversely with $ln$ $K$ values (Figure 5-11). At low hydraulic conductivities, the trends observed are intuitive; PCE is retarded more than TCE which is, in turn, retarded more than DCE.

The values of $A_{11}$, and the parameter $\zeta$ used to calculate it, are included in Table 5-9. It is evident that for the more strongly sorbing PCE, the retarded longitudinal

55

macrodispersivity, $A_{11}$, increased (over $A_o$, the conservative macrodispersivity) by a factor of 2.1. This is an important consideration in the modeling or understanding of the transport of this compound. For the least sorptive compound DCE, the velocity variances introduced by sorption were small as reflected by a small increase in the longitudinal macrodispersivity (factor of 1.2). The macrodispersivity numbers were evaluated using the theoretical distribution coefficients for DCE, TCE, and PCE.

Table 5-9. Values of the retarded longitudinal macrodispersivity, $A_{11}$ and the parameters used in its calculation. All of the parameters have been defined in the text.

| Compound | $\overline{R}$ | $\zeta$ | $A_{11}$ (m) |
|----------|------|------|----------|
| DCE | 1.04 | 0.72 | 24 |
| TCE | 1.10 | 0.75 | 29 |
| PCE | 1.25 | 0.76 | 41 |

In a field setting, neglecting macrodispersivity in the modeling of contaminants can lead to erroneous conclusions. For example, if PCE has arrived at a monitoring well as fast as DCE is observed, then the obvious conclusion may be that retardation is insignificant in this aquifer. However, if one considers the values calculated above, it is easy to see why the PCE may have arrived earlier than expected. The retarded longitudinal macrodispersivity, in effect, quantifies the extent of a mixing zone in front of the leading edge of a contaminant plume. These effects become more visible with an example. Assuming a pulse input of contaminants, the concentration of any solute at any point downstream of the source can be determined from,

$$C = \frac{M}{nA\sqrt{4\pi A_{11}v}}\exp-\left[\frac{(x-vt)^2}{4A_{11}v}\right] \qquad (5\text{-}13)$$

where $C$ is the concentration at any point in the aquifer, $M$ is the initial mass input of contaminants, $x$ is the distance downstream of the input, $t$ is the time at which concentrations are evaluated, $A$ is the cross-sectional area of flow, and $v$ is the advection velocity (adjusted by the proper retardation factors). Using this expression, the normalized concentration of solutes at any time can be predicted as a function of distance (Figure 5-12).
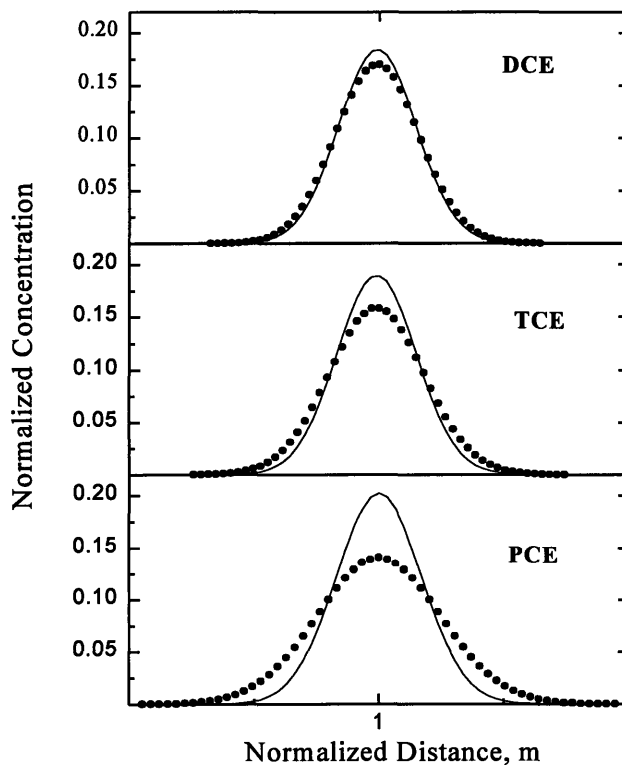


Figure 5-12. Normalized concentrations of three solutes (DCE, TCE, and PCE) as a function of normalized distance from a hypothetical source. Each of the plots is normalized to their respective distances where concentration peaks occur. The solid lines represent concentrations with conservative macrodispersivity values ($R = 1$). The points represent values obtained with retarded macrodispersivity values. The more strongly sorbing PCE disperses more because of field-scale heterogeneity and the velocity variances introduced by sorption.

This figure was generated assuming a contaminant travel distance of 12,000 ft which is consistent with the CS-4 plume analyzed in this study (Lazaro, 1996). Using this travel distance, a travel time was calculated and the concentrations in the aquifer were calculated for this specific time. The relative positions of the solutes in the aquifer would be different because of different retardation and longitudinal macrodispersivity values. The solid lines in each case, represent the concentration distribution of each respective compound using $A_{11}$ equal to $A_o$ (the conservative longitudinal macrodispersivity value). The points represent calculations for the concentrations of the compounds with their respective retarded longitudinal macrodispersivity, $A_{11}$. It is evident that the more sorptive compound (i.e., PCE) experiences larger dispersion and the "mixing zone" for PCE is larger than the other compounds. This is an important consideration in the transport modeling of contaminants. Careful examination of the macrodispersive properties of each solute is necessary to facilitate the quantification of this phenomenon. For these calculations, retardation factors that are paired up with hydraulic conductivity values were necessary.

### 5.3.3 Bioavailability of Contaminants

The sorption of solutes has other effects on contaminants. For example, a factor that needs to be considered is that bioremediation schemes have to account for this retardation. If a multi-phase reactor setup is used to model the degradation of the contaminants, the output from each of these phases needs to be adjusted according to the retardation of the contaminants. For example, if phase one of the reactor is aimed at degrading PCE to TCE, this new mass of TCE will sorb onto the solid. This resulting modified aqueous concentration is the input to the next phase. The bioremediation scheme will have to be designed based on this modified maximum concentration. The initial concentration of the contaminants are not of concern and do not appear in the kinetic expressions when the concentrations are low. At higher concentrations, the degradation process can introduce products that are toxic to the methanotrophs and this

toxicity effect is incorporated in the kinetic expressions (Skiadas, 1996). Retardation can reduce the toxicity of these compounds by reducing their aqueous concentrations.

# 6. Conclusions

This study was undertaken to quantify the sorption of some chlorinated solvents in the Western Cape Cod aquifer. Equilibrium batch sorption studies were used and compared to theoretically derived values to assess the use of theoretical values to quantify field-scale sorption. Once this relationship was established, the uptake behavior was used, in conjunction with other site characterization parameters, to model the transport of the contaminants (i.e., sorption effects on macrodispersion). Sorption was also used to assess the bioavailability of contaminants in the Cape Cod aquifer. The results of this study indicate the following:

- Site characterization efforts should be augmented so that they take into account sorption of contaminants. Batch tests are important in assessing maximum possible sorption uptake. Column tests should, however, represent aquifer conditions better and might present a better alternative to batch tests.

- Theoretical distribution coefficients were in agreement with experimentally derived values. This suggests that theoretical coefficients may be used to assess the behavior of certain solutes.

- Enhanced macrodispersivity due to velocity variations introduced by sorption needs to be considered. Larger dispersivities can result in faster apparent travel velocities of contaminants. This may be of concern if containment of contaminants is desired

- The bioavailability and toxicity of contaminants may be reduced because of sorptive uptake.

It is important to quantify sorption for the assessment of contaminant fate. Theoretically derived values are insufficient in describing field-scale properties of contaminants. Care should be taken in extrapolating laboratory results to field-scale phenomenon. Ideally,

field measurements (i.e., tracer studies, etc.) would present the best possible situation for the quantification of sorption.

# References

ABB Environmental Services Inc. *Groundwater Focused Feasibility Study West Truck Road Motor Pool (AOC CS-4)*, Installation Restoration Program, Massachusetts Military Reservation, prepared for HAZWRAP; Portland ME, February 1992a.

ABB Environmental Services Inc. *Record of Decision Interim Remedial Action West Truck Road Motor Pool (AOC CS-4) Groundwater Operable Unit*, Installation Restoration Program, Massachusetts Military Reservation, prepared for HAZWRAP; Portland ME, May 1992b.

ABB Environmental Services Inc. *CS-4 Groundwater Operable Unit. Extraction and Treatment System. Final Design Package, Volume I, Drawings and Technical Specifications*, Installation Restoration Program, Massachusetts Military Reservation, prepared for HAZWRAP, Portland ME, July 1992c.

ABB Environmental Services Inc. *Personal communication*, March, 1996

Ahlfeld, D. P., and C. S. Sawyer, "Well location in capture zone design using simulation and optimization techniques", *Ground Water*, 28(4), 507-512, 1990.

Bartow, G., and C. Davenport, "Pump-and-treat accomplishments: A review of the effectiveness of ground water remediation in Santa Clara Valley, California", *GWMR*, Spring, 140-146, 1995.

Ball , W. P. and P. V. Roberts, "Long-term sorption of halogenated organic chemicals by aquifer material. 1. Equilibrium," *Environ. Sci. Technol.*, 25, 1223-1236 (1991).

Ball , W. P. and P. V. Roberts, "Long-term sorption of halogenated organic chemicals by aquifer material. 2. Intraparticle Diffusion ," *Environ. Sci. Technol.*, 25, 1223-1236 (1991).

Barber II, L. B., E. M. Thurman, M. P. Schroeder, and D. R. LeBlanc, "Long-term fate of organic micropollutants in sewage contaminated ground water," *Environ. Sci. Technol.*, 22, 205-211(1988).

Barber II, L.B., E.M. Thurman, and D.D. Runnells, "Geochemical heterogeneity in a sand and gravel aquifer: Effect of sediment mineralogy and particle size on the sorption of chlorobenzenes," *J. Contam. Hydrol.*, 9, 35-54 (1992).

Cape Cod Commission. *Cape Trends, Demographic and Economic Characteristics and Trends; Barnstable County- Cape Cod*, 3rd. Ed., Barnstable MA, 1996.

Chiou, C.T., L.J. Peters, and V.H. Freed, "A physical concept of soil-water equilibria for nonionic compounds,' *Science*, **206**, 831-832 (1979).

Collins, Michael. *Design of a Sequential In-Situ Anaerobic/Aerobic Enhanced Bioremediation System for a Chlorinated Solvent contaminated Plume*. Master of Engineering Thesis, Department of Civil and Environmental Engineering, Massachusetts Institute of Technology, Cambridge, 1996.

Cookson, John T. *Bioremediation Engineering: Design and Application*. McGraw Hill, 1995.

E.C. Jordan Co. *Site Inspection Report, Field Investigation Report Conducted Fall 1987, Task 2-3A*, Installation Restoration Program, Massachusetts Military Reservation, prepared for HAZWRAP, Portland ME, March 1989a.

E.C. Jordan Co. *Hydrogeologic Summary Report, Task 1-8*, Installation Restoration Program, Massachusetts Military Reservation, prepared for HAZWRAP, Portland ME, April 1989b.

E.C. Jordan Co. *Groundwater Feasibility Study, Study Area CS-4*, Installation Restoration Program, Massachusetts Military Reservation, prepared for HAZWRAP, Portland ME; October 1990.

Foster-Reid, G. H., *Variability of Hydraulic Conductivity and Sorption in a Heterogeneous Aquifer*, M.S. Thesis, Department of Civil and Environmental Engineering, Massachusetts Institute of Technology, Cambridge, 1994.

Garabedian, S.P., Gelhar, L.W., and Celia, M.A. *Large-Scale Dispersive Transport in Aquifers: Field Experiments and Reactive Transport Theory*, Report 315, Ralph M. Parsons Laboratory, Department of Civil and Environmental Engineering, Massachusetts Institute of Technology, Cambridge MA, 1988.

Gauthier T.D., E.C. Shane, W. F. Guerin, W. R. Seitz, and C. L. Grant, "Fluorescence Quenching Method for Determining Equilibrium Constants for Polycyclic Aromatic Hydrocarbons Binding to Dissolved Humic Materials", *Environmental Science and Technology*, 20(11), 1162-1166, 1986.

Gelhar, L.W. and C.L. Axness, "Three-dimensional stochastic analysis of macrodispersion in aquifers", *Water Resources Research*, 19(1), 161-180, 1983.

Gelhar, L. W., Welty, C., and Rehfeldt, K. R., "A critical review of data on field-scale dispersion in aquifers," *Water Resources Research*, 28(7), 1955-1974, 1992.

Gelhar, L.W., *Stochastic Subsurface Hydrology*, Prentice Hall, New York, 1993.

Gu, B, J., Schmitt, and Z. Chen, "Adsorption and desorption of natural organic matter on iron oxide : mechanisms and models", *Environmental Science and Technology*, 28, 38-46, 1994.

Guswa, J. H., and LeBlanc, D. R. *Digital Models of Groundwater Flow in the Cape Cod Aquifer System, Massachusetts*, U.S. Geological Survey, Water Supply Paper, 1985.

Hansch, C., A. Leo, and D.H. Hoekman, *Exploring QSAR*, American Chemical Society, 1995.

Hatzinger, P. B. and M. Alexander, "Effect of Aging of Chemicals in Soil on Their Biodegradability and Extractability", *Environmental Science and Technology*, 29(2), 537-545, 1995.

Hayes, Michael F. Jr. *Stimulating In Situ groundwater Bioremediation via Sparging: Gas Flow, Groundwater Flow, and Mass Transfer in the Biosparge Zone*, M.S Thesis, Department of Civil and Environmental Engineering, Massachusetts Institute of Technology, 1996.

Hoffman, F., "Smart pump and treat," *Ground Water*, 31(1), 98-102, 1993.

Holmén, B.A., *Polycyclic Aromatic Hydrocarbon Sorption Kinetics in Three Iron Oxide-Coated Aquifer Sands*, Ph.D. Dissertation, Massachusetts Institute of Technology (1995).

Jardine, P. M., N. L. Weber and J. F. McCarthy, "Mechanisms of dissolved organic carbon adsorption on soil," *Soil Sci. Soc. Am. J.*, 53, 1378-1385 (1989).

Karickhoff, S. W., D. S. Brown, and T. A. Scott, "Sorption of hydrophobic pollutants on natural sediments," Water Res. **13**, 241-248 (1979)

Karickhoff, S. W., "Semi-empirical estimation of sorption of hydrophobic pollutants on natural sediments and soils," *Chemosphere*, **10**, 833-846 (1981).

Lázaro, A. M., *Simulation of Groundwater Contaminant Plume in a Sand and Gravel Aquifer in Cape Cod, Massachusetts Using a 3D Model*, Master of Engineering Thesis, Department of Civil and Environmental Engineering, Massachusetts Institute of Technology, Cambridge, 1996.

LeBlanc, D. R., Guswa, J. H., Frimpter, M. H., and Londquist, C. J. *Ground-Water Resources of Cape Cod, Massachusetts*, Hydrological Investigation Atlas, HA-692, 4 sheets, U.S. Geological Survey, Reston, Va., 1986.

LeBlanc, D. R., Garabedian, S. P., Hess, K. M., Gelhar, L. W., Quadri, R. D., Stollenwerk, K. G., and Wood, W. W., "Large-scale natural gradient tracer test in

sand and gravel, Cape Cod, Massachusetts. Section 1: Experimental design and observed rracer movement," *Water Resources Research*, 27(5), 895-910, 1991.

Lopez-Calva, Enrique, *Analysis of Pumping Schemes for the Extraction of Contaminated Groundwater, at Cape Cod, Massachusetts, Using 3-D Numerical Modeling*. Master of Engineering thesis, Massachusetts Institute of Technology. Cambridge. 1996

MacDonald, J. A. and Kavanaugh, M. C. , "Restoring Contaminated Groundwater: An Achievable Goal?," *Environmental Science and Technology*, 28(8), 362-368, 1994.

Mackay, D. M. and Cherry, J. A., "Groundwater contamination: Pump-and treat remediation," *Environmental Science and Technology*, 23(6), 630-636, 1989.

Massachusetts Executive Office of Environmental Affairs. *Water Resources of Cape Cod: Water Use, Hydrology, and Potential Changes in Ground Water Levels*, Department of Environmental Management, Office of Water Resources, October 1994.

Masterson J. P. and P. M. Barlow, "Effects of Simulated Ground-Water Pumping and Recharge on Ground-Water Flow in Cape Cod, Martha's Vineyard, and Nantucket Island Basins, Massachusetts", U.S. Geological Survey, Open-File Report 94-316, 1994.

Means J. C., S. G. Wood, J. J. Hassett, W.L. Banwart, "Sorption of Polynuclear Aromatic Hydrocarbons by Sediments and Soils", *Environmental Science and Technology*, 14(12), 1524-1528, 1980.

Oldale, R. N. Pleistocene Stratigraphy of Nantucket, Martha's Vineyard, the Elizabeth Islands, and Cape Cod, Massachusetts, in *Wisconsian Glaciation of New England*, edited by G. J. Larson and B. D. Stone, pp. 1-34, Kendall/Hunt, Dubuque, Iowa, 1982.

Oldale, R. N., and Barlow, R. A. Geologic Map of Cape Cod and the Island, Massachusetts, *Misc. Invest. Ser., Map I-1763*, U.S. Geological Survey, Reston, VA, 1987.

Parks, G. A., "The isoelectric points of solid oxides, solid hydroxides, and aqueous hydroxo complex systems," *Chem. Rev.*, **65**, 177-198 (1965).

Piatt, J. J., D. A. Backhus, and P. D. Capel, "Temperature-dependent sorption of naphthalene, phenanthrene, and pyrene to low organic carbon aquifer sediments", *Environmental Science and Technology*, 30, 751-760, 1996.

Picazo, C. L., *Human Health Risk Assessment of Chemical Spill 4 at the Massachusetts Military Reservation*. Master of Engineering thesis, Massachusetts Institute of Technology. Cambridge. 1996

Rajaram, H. and Gelhar, L.W., "Plume-scale dependent dispersion in aquifers with a wide range of scales of heterogeneity," *Water Resources Research*, 31(10), 2469-2482, 1995.

Schwarzenbach, R.P. and J. Westall, "Transport of nonpolar organic compounds from surface water to groundwater. Laboratory sorption studies," *Environ. Sci. Technol.*, **15**, 1360-1367 (1981).

Schwarzenbach, R. P., P. M. Gschwend, and D. M. Imboden, *Environmental Organic Chemistry*, Wiley, New York, 1993.

Semprini, Lewis; Hopkins, G. D.; Roberts, P. V.; McCarty, P. L., "A field evaluation of in situ biodegradation of chlorinated ethenes: Part 3. Studies of competitive inhibition," *Ground Water*, Vol. 29(2), pp. 239-250, 1991a.

Semprini, Lewis; McCarty, P. L., "Comparison between model simulations and field results for in situ biorestoration of chlorinated aliphatics: Part 1. Biostimulation of methanotrophic bacteria," *Ground Water*, Vol. 29(3), pp. 365-374, 1991b.

Skiadas, Panagiotis. *Design of an In Situ Bioremediation Scheme of Chlorinated Solvents by Reductive Dehalogenation Sequenced by Cometabolic Oxidation.* Master of Engineering Thesis. Massachusetts Institute of Technology. Cambridge, MA 1996.

Stenzel, Mark H., Merz, William J., "Use of Carbon Adsorption Processes in groundwater treatment," *Environmental Progress*, 8(4), 1989.

Talbott, M. E. and L. W. Gelhar, "Performance Assessment of a Hypothetical Low-Level Waste Facility", Prepared for U.S. Nuclear Regulatory Commission, Division of Regulatory Applications, NUREG/CR-6114, May 1994.

Thompson, K. D., *The Stochastic Characterization of Glacial Aquifers Using Geologic Information*, Ph.D. Thesis, Department of Civil and Environmental Engineering, Massachusetts Institute of Technology, Cambridge, 1994.

Tillman, D. E., *Combination of zero-valent iron and granular activated carbon for the treatment of groundwater contaminated with chlorinated solvents*, Master of Engineering Thesis, Department of Civil and Environmental Engineering, Massachusetts Institute of Technology, Cambridge, 1996.

Travis, C. C. and Doty, C. B. Can Contaminated Aquifers at Superfund Sites be Remediated? *Environmental Science and Technology*, 24(10), 1464-1466, 1990.

Vo-Dinh, T., "Synchronous Excitation Spectroscopy" In *Modern Fluorescence Spectroscopy*, E.L. Wehry (Ed.), Plenum Press, New York, N.Y., 1981.

# Appendix A : Laboratory Data

## PHENANTHRENE DATA

| Sample ID | % Solubility in vial | Fluorescence of Vial w/o Sorption | Aqueous Fluorescence @ Equilibrium | Adjusted Aqueous Fluorescence (for Teflon) | "Fluorescence" of Sorbed Pyrene | $C_w$ (moles/L) | $C_s$ (moles/kg) |
|---|---|---|---|---|---|---|---|
| 1810 | 7.31 | 43.55 | 41.44 | 45.80 | -2.24 | 4.53E-07 | 1.94E-06 |
| 1820 | 14.62 | 159.04 | 90.09 | 99.56 | 59.48 | 6.47E-07 | 3.66E-06 |
| 1830 | 21.94 | 274.52 | 150.85 | 166.72 | 107.81 | 8.90E-07 | 5.01E-06 |
| 1840 | 29.25 | 390.00 | 223.44 | 246.93 | 143.07 | 1.18E-06 | 5.99E-06 |
| 1850 | 36.56 | 505.49 | 276.80 | 305.91 | 199.58 | 1.39E-06 | 7.56E-06 |
| 1860 | 43.87 | 620.97 | 324.09 | 358.17 | 262.80 | 1.58E-06 | 9.32E-06 |
| 1811 | 7.31 | 43.55 | 46.92 | 51.85 | -8.30 | 4.75E-07 | 1.77E-06 |
| 1821 | 14.62 | 159.04 | 113.50 | 125.44 | 33.60 | 7.41E-07 | 2.94E-06 |
| 1831 | 21.94 | 274.52 | 141.53 | 156.41 | 118.11 | 8.53E-07 | 5.29E-06 |
| 1841 | 29.25 | 390.00 | 232.18 | 256.60 | 133.40 | 1.21E-06 | 5.72E-06 |
| 1851 | 36.56 | 505.49 | 282.39 | 312.08 | 193.40 | 1.42E-06 | 7.39E-06 |
| 1861 | 43.87 | 620.97 | 315.57 | 348.76 | 272.21 | 1.55E-06 | 9.59E-06 |
| 5810 | 8.63 | 64.28 | 63.41 | 70.08 | -5.80 | 5.41E-07 | 4.40E-07 |
| 5820 | 17.25 | 200.50 | 132.20 | 146.10 | 54.40 | 8.16E-07 | 8.41E-07 |
| 5830 | 25.88 | 336.71 | 181.81 | 200.94 | 135.78 | 1.01E-06 | 1.38E-06 |
| 5840 | 34.50 | 472.93 | 275.98 | 305.00 | 167.92 | 1.39E-06 | 1.60E-06 |
| 5850 | 43.13 | 609.14 | 318.91 | 352.45 | 256.69 | 1.56E-06 | 2.19E-06 |
| 5860 | 51.75 | 745.36 | 366.28 | 404.80 | 340.56 | 1.75E-06 | 2.75E-06 |
| 5811 | 8.63 | 64.28 | 47.85 | 52.88 | 11.41 | 4.79E-07 | 5.55E-07 |
| 5821 | 17.25 | 200.50 | 130.18 | 143.87 | 56.63 | 8.07E-07 | 8.56E-07 |
| 5831 | 25.88 | 336.71 | 205.78 | 227.42 | 109.29 | 1.11E-06 | 1.21E-06 |
| 5841 | 34.50 | 472.93 | 275.42 | 304.38 | 168.54 | 1.39E-06 | 1.60E-06 |
| 5851 | 43.13 | 609.14 | 302.63 | 334.46 | 274.68 | 1.50E-06 | 2.31E-06 |
| 5861 | 51.75 | 745.36 | 371.20 | 410.24 | 335.12 | 1.77E-06 | 2.71E-06 |

## PHENANTHRENE DATA

| Sample ID | % Solubility in vial | Fluorescence of Vial w/o Sorption | Aqueous Fluorescence @ Equilibrium | Adjust Aqueous Fluorescence (for Teflon) | "Fluorescence" of Sorbed Pyrene | $C_w$ (moles/L) | $C_s$ (moles/kg) |
|---|---|---|---|---|---|---|---|
| 7310 | 9.66 | 80.66 | 75.67 | 83.63 | -2.98 | 5.90E-07 | 2.87E-07 |
| 7320 | 19.32 | 233.24 | 148.67 | 164.30 | 68.94 | 8.81E-07 | 5.86E-07 |
| 7330 | 28.98 | 385.83 | 216.36 | 239.11 | 146.71 | 1.15E-06 | 9.09E-07 |
| 7340 | 38.65 | 538.41 | 311.15 | 343.87 | 194.54 | 1.53E-06 | 1.11E-06 |
| 7350 | 48.31 | 691.00 | 367.41 | 406.05 | 284.95 | 1.76E-06 | 1.48E-06 |
| 7360 | 57.97 | 843.58 | 448.89 | 496.11 | 347.48 | 2.08E-06 | 1.74E-06 |
| 7311 | 9.66 | 80.66 | 71.81 | 79.36 | 1.30 | 5.74E-07 | 3.05E-07 |
| 7321 | 19.32 | 233.24 | 166.11 | 183.58 | 49.66 | 9.51E-07 | 5.06E-07 |
| 7331 | 28.98 | 385.83 | 230.76 | 255.03 | 130.80 | 1.21E-06 | 8.43E-07 |
| 7341 | 38.65 | 538.41 | 279.81 | 309.24 | 229.18 | 1.41E-06 | 1.25E-06 |
| 7351 | 48.31 | 691.00 | 391.54 | 432.72 | 258.28 | 1.85E-06 | 1.37E-06 |
| 7361 | 57.97 | 843.58 | 389.64 | 430.62 | 412.96 | 1.84E-06 | 2.02E-06 |
| 7810 | 10.16 | 88.45 | 62.82 | 69.43 | 19.02 | 5.38E-07 | 3.21E-07 |
| 7820 | 20.31 | 248.84 | 139.49 | 154.16 | 94.68 | 8.45E-07 | 5.88E-07 |
| 7830 | 30.47 | 409.22 | 187.07 | 206.74 | 202.48 | 1.03E-06 | 9.68E-07 |
| 7840 | 40.62 | 569.60 | 265.66 | 293.60 | 276.01 | 1.35E-06 | 1.23E-06 |
| 7850 | 50.78 | 729.99 | 333.26 | 368.31 | 361.67 | 1.62E-06 | 1.53E-06 |
| 7860 | 60.93 | 890.37 | 427.06 | 471.98 | 418.39 | 1.99E-06 | 1.73E-06 |
| 7811 | 10.16 | 88.45 | 43.11 | 47.64 | 40.81 | 4.60E-07 | 3.98E-07 |
| 7821 | 20.31 | 248.84 | 152.46 | 168.49 | 80.34 | 8.96E-07 | 5.37E-07 |
| 7831 | 30.47 | 409.22 | 154.50 | 170.75 | 238.47 | 9.05E-07 | 1.10E-06 |
| 7841 | 40.62 | 569.60 | 289.96 | 320.45 | 249.15 | 1.45E-06 | 1.13E-06 |
| 7851 | 50.78 | 729.99 | 351.19 | 388.12 | 341.87 | 1.69E-06 | 1.46E-06 |
| 7861 | 60.93 | 890.37 | 383.91 | 424.28 | 466.09 | 1.82E-06 | 1.90E-06 |

**PHENANTHRENE DATA**

| Sample ID | % Solubility in vial | Fluorescence of Vial w/o Sorption | Aqueous Fluorescence @ Equilibrium | Adjust Aqueous Fluorescence (for Teflon) | "Fluorescence" of Sorbed Pyrene | $C_w$ (moles/L) | $C_s$ (moles/kg) |
|---|---|---|---|---|---|---|---|
| 8810 | 9.07 | 71.24 | 57.15 | 63.16 | 8.08 | 5.16E-07 | 4.24E-07 |
| 8820 | 18.13 | 214.42 | 147.27 | 162.76 | 51.66 | 8.76E-07 | 6.55E-07 |
| 8830 | 27.20 | 357.59 | 206.77 | 228.52 | 129.08 | 1.11E-06 | 1.07E-06 |
| 8840 | 36.26 | 500.77 | 294.03 | 324.96 | 175.81 | 1.46E-06 | 1.31E-06 |
| 8850 | 45.33 | 643.94 | 385.98 | 426.58 | 217.37 | 1.83E-06 | 1.53E-06 |
| 8860 | 54.39 | 787.12 | 428.73 | 473.82 | 313.30 | 2.00E-06 | 2.04E-06 |
| 8811 | 9.07 | 71.24 | 46.67 | 51.58 | 19.66 | 4.74E-07 | 4.86E-07 |
| 8821 | 18.13 | 214.42 | 134.75 | 148.93 | 65.49 | 8.26E-07 | 7.29E-07 |
| 8831 | 27.20 | 357.59 | 190.25 | 210.26 | 147.34 | 1.05E-06 | 1.16E-06 |
| 8841 | 36.26 | 500.77 | 287.52 | 317.76 | 183.01 | 1.44E-06 | 1.35E-06 |
| 8851 | 45.33 | 643.94 | 367.74 | 406.42 | 237.53 | 1.76E-06 | 1.64E-06 |
| 8861 | 54.39 | 787.12 | 449.43 | 496.70 | 290.42 | 2.08E-06 | 1.92E-06 |

## PYRENE DATA

| Sample ID | % Solubility in vial | Fluorescence of Vial w/o Sorption | Aqueous Fluorescence @ Equilibrium | Adjust Aqueous Fluorescence (for Teflon) | "Fluorescence" of Sorbed Pyrene | $C_w$ (moles/L) | $C_s$ (moles/kg) |
|---|---|---|---|---|---|---|---|
| 1810 | 8.48 | 94.09 | 17.3 | 20.66 | 73.44 | 3.29E-08 | 3.54E-07 |
| 1820 | 16.96 | 274.76 | 43.1 | 51.55 | 223.20 | 4.11E-08 | 6.85E-07 |
| 1830 | 25.43 | 455.42 | 80.9 | 96.84 | 358.58 | 5.31E-08 | 9.85E-07 |
| 1840 | 33.91 | 636.09 | 139.8 | 167.34 | 468.75 | 7.18E-08 | 1.23E-06 |
| 1850 | 42.39 | 816.75 | 146.4 | 175.21 | 641.54 | 7.39E-08 | 1.61E-06 |
| 1860 | 50.87 | 997.42 | 171.8 | 205.64 | 791.78 | 8.20E-08 | 1.94E-06 |
| | | | | | | | |
| 1811 | 8.48 | 94.09 | 24.0 | 28.75 | 65.34 | 3.51E-08 | 3.36E-07 |
| 1821 | 16.96 | 274.76 | 59.5 | 71.28 | 203.47 | 4.64E-08 | 6.42E-07 |
| 1831 | 25.43 | 455.42 | 72.5 | 86.84 | 368.58 | 5.05E-08 | 1.01E-06 |
| 1841 | 33.91 | 636.09 | 130.3 | 156.04 | 480.05 | 6.88E-08 | 1.25E-06 |
| 1851 | 42.39 | 816.75 | 154.0 | 184.39 | 632.37 | 7.63E-08 | 1.59E-06 |
| 1861 | 50.87 | 997.42 | 170.7 | 204.42 | 793.00 | 8.16E-08 | 1.95E-06 |
| | | | | | | | |
| 5810 | 10.00 | 126.53 | 32.7 | 39.15 | 87.38 | 3.78E-08 | 9.20E-08 |
| 5820 | 20.00 | 339.63 | 63.4 | 75.90 | 263.73 | 4.76E-08 | 1.85E-07 |
| 5830 | 30.00 | 552.73 | 105.2 | 125.90 | 426.83 | 6.08E-08 | 2.71E-07 |
| 5840 | 40.00 | 765.83 | 175.0 | 209.48 | 556.35 | 8.30E-08 | 3.40E-07 |
| 5850 | 50.00 | 978.93 | 188.5 | 225.64 | 753.29 | 8.73E-08 | 4.44E-07 |
| 5860 | 60.00 | 1192.03 | 216.2 | 258.86 | 933.17 | 9.61E-08 | 5.39E-07 |
| | | | | | | | |
| 5811 | 10.00 | 126.53 | 19.1 | 22.89 | 103.64 | 3.35E-08 | 1.01E-07 |
| 5821 | 20.00 | 339.63 | 66.9 | 80.07 | 259.56 | 4.87E-08 | 1.83E-07 |
| 5831 | 30.00 | 552.73 | 111.1 | 132.98 | 419.75 | 6.27E-08 | 2.68E-07 |
| 5841 | 40.00 | 765.83 | 155.2 | 185.77 | 580.06 | 7.67E-08 | 3.52E-07 |
| 5851 | 50.00 | 978.93 | 170.3 | 203.89 | 775.04 | 8.15E-08 | 4.56E-07 |
| 5861 | 60.00 | 1192.03 | 197.1 | 236.00 | 956.03 | 9.00E-08 | 5.51E-07 |

# PYRENE DATA

| Sample ID | % Solubility in vial | Fluorescence of Vial w/o Sorption | Aqueous Fluorescence @ Equilibrium | Adjust Aqueous Fluorescence (for Teflon) | "Fluorescence" of Sorbed Pyrene | $C_w$ (moles/L) | $C_s$ (moles/kg) |
|---|---|---|---|---|---|---|---|
| 7310 | 11.20 | 152.14 | 48.8 | 58.44 | 93.70 | 4.30E-08 | 5.95E-08 |
| 7320 | 22.40 | 390.85 | 89.5 | 107.12 | 283.74 | 5.59E-08 | 1.22E-07 |
| 7330 | 33.61 | 629.57 | 136.1 | 162.96 | 466.61 | 7.06E-08 | 1.83E-07 |
| 7340 | 44.81 | 868.28 | 195.2 | 233.71 | 634.57 | 8.94E-08 | 2.38E-07 |
| 7350 | 56.01 | 1106.99 | 221.3 | 264.93 | 842.06 | 9.77E-08 | 3.07E-07 |
| 7360 | 67.21 | 1345.70 | 278.9 | 333.89 | 1011.81 | 1.16E-07 | 3.63E-07 |
| 7311 | 11.20 | 152.14 | 42.1 | 50.43 | 101.71 | 4.08E-08 | 6.22E-08 |
| 7321 | 22.40 | 390.85 | 110.7 | 132.53 | 258.32 | 6.26E-08 | 1.14E-07 |
| 7331 | 33.61 | 629.57 | 145.9 | 174.66 | 454.90 | 7.38E-08 | 1.79E-07 |
| 7341 | 44.81 | 868.28 | 163.1 | 195.29 | 672.99 | 7.92E-08 | 2.51E-07 |
| 7351 | 56.01 | 1106.99 | 243.7 | 291.74 | 815.25 | 1.05E-07 | 2.98E-07 |
| 7361 | 67.21 | 1345.70 | 226.3 | 270.94 | 1074.77 | 9.93E-08 | 3.84E-07 |
| 7810 | 11.77 | 164.34 | 32.3 | 38.69 | 125.65 | 3.77E-08 | 5.95E-08 |
| 7820 | 23.55 | 415.25 | 79.1 | 94.69 | 320.56 | 5.26E-08 | 1.14E-07 |
| 7830 | 35.32 | 666.16 | 99.2 | 118.82 | 547.34 | 5.90E-08 | 1.78E-07 |
| 7840 | 47.10 | 917.07 | 142.4 | 170.46 | 746.61 | 7.26E-08 | 2.33E-07 |
| 7850 | 58.87 | 1167.98 | 190.4 | 228.01 | 939.98 | 8.79E-08 | 2.88E-07 |
| 7860 | 70.65 | 1418.90 | 239.1 | 286.30 | 1132.60 | 1.03E-07 | 3.42E-07 |
| 7811 | 11.77 | 164.34 | 19.8 | 23.72 | 140.63 | 3.37E-08 | 6.37E-08 |
| 7821 | 23.55 | 415.25 | 88.6 | 106.07 | 309.18 | 5.56E-08 | 1.11E-07 |
| 7831 | 35.32 | 666.16 | 81.7 | 97.78 | 568.39 | 5.34E-08 | 1.84E-07 |
| 7841 | 47.10 | 917.07 | 167.6 | 200.63 | 716.44 | 8.06E-08 | 2.25E-07 |
| 7851 | 58.87 | 1167.98 | 189.3 | 226.64 | 941.35 | 8.75E-08 | 2.88E-07 |
| 7861 | 70.65 | 1418.90 | 214.2 | 256.45 | 1162.44 | 9.54E-08 | 3.50E-07 |

# PYRENE DATA

| Sample ID | % Solubility in vial | Fluorescence of Vial w/o Sorption | Aqueous Fluorescence @ Equilibrium | Adjust Aqueous Fluorescence (for Teflon) | "Fluorescence" of Sorbed Pyrene | $C_w$ (moles/L) | $C_s$ (moles/kg) |
|---|---|---|---|---|---|---|---|
| 8810 | 10.51 | 137.42 | 47.6 | 57.01 | 80.41 | 4.26E-08 | 7.03E-08 |
| 8820 | 21.02 | 361.41 | 125.9 | 150.69 | 210.72 | 6.74E-08 | 1.25E-07 |
| 8830 | 31.53 | 585.39 | 129.6 | 155.21 | 430.19 | 6.86E-08 | 2.18E-07 |
| 8840 | 42.04 | 809.38 | 266.3 | 318.81 | 490.57 | 1.12E-07 | 2.43E-07 |
| 8850 | 52.55 | 1033.37 | 257.3 | 308.08 | 725.29 | 1.09E-07 | 3.42E-07 |
| 8860 | 63.07 | 1257.36 | 270.6 | 324.02 | 933.34 | 1.13E-07 | 4.30E-07 |
| 8811 | 10.51 | 137.42 | 22.5 | 26.92 | 110.50 | 3.46E-08 | 8.30E-08 |
| 8821 | 21.02 | 361.41 | 83.1 | 99.52 | 261.89 | 5.38E-08 | 1.47E-07 |
| 8831 | 31.53 | 585.39 | 120.3 | 144.00 | 441.40 | 6.56E-08 | 2.22E-07 |
| 8841 | 42.04 | 809.38 | 174.3 | 208.70 | 600.68 | 8.28E-08 | 2.89E-07 |
| 8851 | 52.55 | 1033.37 | 233.7 | 279.82 | 753.55 | 1.02E-07 | 3.54E-07 |
| 8861 | 63.07 | 1257.36 | 319.2 | 382.19 | 875.17 | 1.29E-07 | 4.05E-07 |

# Appendix B : Project Results

## Project Executive Summary

This appendix covers the technical aspects of the current situation of the Chemical Spill 4 (CS-4) groundwater plume at the Massachusetts Military Reservation (MMR), and proposes a final remedial design.

The aquifer underlying the MMR is contaminated by various pollutants forming a plume. The CS-4 plume is currently contained using a pump and treat system. The contaminants of concern detected in CS-4 are perchloroethene (PCE), trichloroethene (TCE), total 1,2-dichloroethene (DCE), and 1,1,2,2-tetrachloroethane (TeCA). Granular activated carbon (GAC) is used to treat the extracted groundwater which is reinjected to the aquifer after treatment. This system was designed as an interim remedial action to quickly respond to the plume migrating off site. A final remedial design must be formulated.

In order to propose a final remedial system for CS-4, the following aspects are examined in depth: (1) an extensive site characterization, (2) the development of a computer model to simulate flow and contaminant transport, (3) the evaluation of the feasibility of bioremediation and its design, (4) the examination of the current aboveground treatment system and possibilities of its enhancing it; and (5) an evaluation of the risk associated with these remedial strategies.

Site characterization was based on previous studies of the area. A three-dimensional model was constructed from the results of the site characterization. The model was used to simulate flow and transport under natural conditions, and to predict effective capture curves for the extraction of the contaminated water. An innovative *in situ* bioremediation system consisting an anaerobic zone sequenced by an aerobic zone was designed. The removal due to biodegradation was calculated. Optimization of the currently operating treatment system was conducted by evaluating economic benefits of combining the existing GAC system with zero-valent iron technology. Risk assessment was performed considering EPA acceptable range of carcinogenic and non-carcinogenic risk.

## Results

### a) Site Characterization

On a regional scale, the geology of western Cape Cod is composed of two glacial moraines deposited along the western and northern edges and a broad outwash plain between the two moraines. The outwash is composed of poorly sorted fine to coarse grained sands, and its thickness varies from approximately 175 feet to 325 feet. Precipitation is the sole source of recharge to the aquifer. Values of recharge are between 18 in/yr and 23 in/yr. A value of 380 ft/day has been accepted as a representative value of average horizontal hydraulic conductivity of the outwash sands. Effective porosity is estimated to be about 0.39 and the average hydraulic gradient is 0.0014.

The groundwater contains high values of dissolved oxygen (5-10 mg/L), and has a pH between 5 and 7. The average temperature is about 13°C. The average concentrations of the main contaminants in CS-4 are 18 ppb, 9.1 ppb, 1.1 ppb and 6.8 ppb for PCE, TCE, DCE and PCA respectively. Previous field observations suggested that the plume is 11,000 ft long, 800 ft wide and 50 ft thick.

### b) Groundwater Model

The groundwater flow model showed great sensitivity to the properties of the glacial moraine. The calibrated model (based on head distributions and particle tracking) has an average hydraulic conductivity of 221.6 ft/day, a hydraulic gradient of 0.0014, a seepage velocity of 0.8 ft/day, and a recharge of 19 in/yr.

*Contaminant Transport Model:*

Simulating a continuous input of the contaminants, the plume resulting from the simulations had greater dimensions than the plume defined by field observations. Average dimensions

were 1,180 ft for the width, 40 ft for the height, and 12,660 ft for the length. These dimensions were defined by the 5 ppb contour interval.

The no action alternative for remediation was simulated. According to the model, the total time it took for all the contaminants to enter the nearest pond would be between 80 to 85 years. On the other hand, the total time for clean-up using the existing system would be approximately 70 years.

*Simulation of Pumping Schemes:*

Simulations using the current 13-well fence indicated that for a plume defined according to the existing field observations, the currently operating pumping scheme is appropriate. The flexibility of the current well fence was tested using a plume 50% larger (in cross-sectional area) that was captured by increasing the overall pumping rate by 78%. Results of different pumping schemes showed that similar capture curves can be obtained with the existing pumping scenario, and with a pumping system of seven wells located 120 ft apart and extracting water at an overall rate of 140 gpm. This seven-well option may be a better option, since presumably, operation and maintenance cost would be reduced.

## c) Bioremediation

The *in situ* bioremediation system consists of three phases. Phase 1 has the objective to create the necessary conditions for reductive dechlorination (phase 2) to take place. Reductive dechlorination is an anaerobic process in which 99 % of PCE was estimated to be transformed to TCE and other less chlorinated ethylenes if given sufficient residence time. In the third phase, TCE, and DCE (and vinyl chloride if produced in phase 2) are degraded by cometabolic oxidation. The degradation fractions were calculated to be 97% for TCE and 100% for DCE and VC.

## d) Aboveground Treatment Alternative

The combination of the existing GAC with the zero-valent iron technology can be an effective means to reduce long-term treatment costs. This can be achieved by installing aboveground reactor vessels filled with zero-valent iron which treats the extracted water before it flows through the GAC. For scenarios in which concentrations of the plume are assumed to be high (maximum concentrations), overall treatment savings up to $200,000 were estimated. For scenarios with low concentrations, no considerable savings can be expected

## e) Risk Assessment

Worst case scenarios using pump and treat result in a carcinogenic risk of $1.4 \times 10^{-6}$. Using bioremediation results in a carcinogenic risk of $2.6 \times 10^{-6}$. The no action alternative results in a carcinogenic risk of $10^{-4}$.

## *Conclusions*

This project was undertaken to fully understand the transport mechanisms of groundwater and contaminants in the western Cape Cod aquifer, and to develop a final remediation scheme for the CS-4 plume. The following conclusions are drawn:

- Site characterization must be improved in order to provide a clearer understanding of the contamination problem. The representation of the aquifer conditions with the computer model was limited because of insufficient data.

- Total clean-up times using the current interim remedial scheme are very long and cost intensive. Development of a final remediation method which decreases clean-up times and decreases costs is necessary.

- Using only seven of the 13 existing wells produces the same results as the current operation. Reexamination of the current pumping scheme would reduce operation and

maintenance costs. It is recommended that this new scheme be examined as an alternative to the existing operation.

- The anaerobic/aerobic *in situ* bioremediation scheme proposed demonstrates that it has the potential to completely degrade PCE, TCE, and DCE. A pilot test is needed to demonstrate the efficacy of this technology and determine the final design parameters.

- By combining the existing GAC with the emerging zero-valent iron technology a reduction in overall treatment costs can be achieved for certain scenarios. A bench-scale study should be conducted to verify the results.

Risk calculations indicate that the CS-4 plume must be remediated to comply with regulations. The remediation strategies reduce the risks to acceptable levels. From a risk standpoint, the preferred strategy is a combination of bioremediation and pump and treat.

# Group Project Results

## *Modeling Under Natural Conditions*

### Description of the Model

A three-dimensional model was constructed using the finite-element modeling code DynSystem (Camp, Dresser & McKee, Inc, 1992). More than 100 wells are located in the area of concern. Data of hydraulic head and contaminant concentrations from the wells were used to construct input files to the model.

The model includes an area of approximately 50 $mi^2$ on the western Cape. The thickness of the modeled region was non-uniform, defined by ground surface and bedrock elevations. The horizontal boundaries were defined by two no-flow boundaries and the ocean. Johns Pond, Ashumet Pond and Childs River were included in the model as fixed head boundary conditions. Coonamessett Pond is the most important surface water body within the modeled area because of its vicinity to the end of the CS-4 plume region.

### Model Recalibration Using Particle Tracking

The calibrated hydrologic flow model was used as the basis for the simulation of contaminant transport in the aquifer. After the first particle run, however, it was evident that the model was not fully calibrated. Even though the heads agreed with the observations, particles went too deep into the aquifer and did not match the field observations. Thus, the model was recalibrated paying special attention to anisotropy ratios, recharge, and the Buzzards Bay Moraine conductivity; (i.e. factors which considerably affected the transport of particles). Table B-1 summarizes the hydraulic parameters in the final calibrated model.

Table B-1: Hydrologic parameters of flow model resulting from the final particle tracking calibration

| Parameter | Value |
|---|---|
| Average Hydraulic Conductivity | 221.6 ft/day |
| Hydraulic Gradient | 0.0014 |
| Seepage Velocity | 0.8 ft/day |
| Anisotropy Ratio | 10:1 and 12.5:1 |
| Recharge | 19 in/yr |
| Head Mean Difference (calc. - obs.) | 0.24 ft |
| Head Standard Deviation | 1.61 ft |

## *Contaminant Transport Modeling*

**Description**

A particle tracking code was used to simulate the movement of particles from the source for a specified amount of time. Particle locations were recorded at the end of each simulation and concentrations were calculated based on particle weight and number of particles per unit volume. A more detailed description of some aspects and outcomes of the transport model is discussed next.

*Source*

A thorough description of the source, its location, dimensions, and input loadings are essential for a reliable model. E.C. Jordan (1989b) provides a thorough description of what is believed to be the CS-4 plume source.

The transport model focuses on the solvents PCE, TCE and DCE. Due to limitations in the program code, they were modeled as one contaminant. Thus, concentration outputs files included the sum of PCE, TCE, and DCE concentrations. The source loading was calibrated

to match the field values. Consequently, the calculated concentrations are compared to the observed values at different well locations.

The source was modeled as a continuous source input of particles. From groundwater velocity data, it was determined that the contamination must have started at least 15 years ago. The source loading was modeled as seven 5 year intervals, from 1960 to 1993 (Figure B-1). The modeled particles were calibrated to observed concentration data. The concentration data was sparse and it was determined that the source loading in Figure B-1 was necessary to adequately model the contaminant plume (to ±30 ppb). For more details on the calibration procedure see Lázaro (1996).
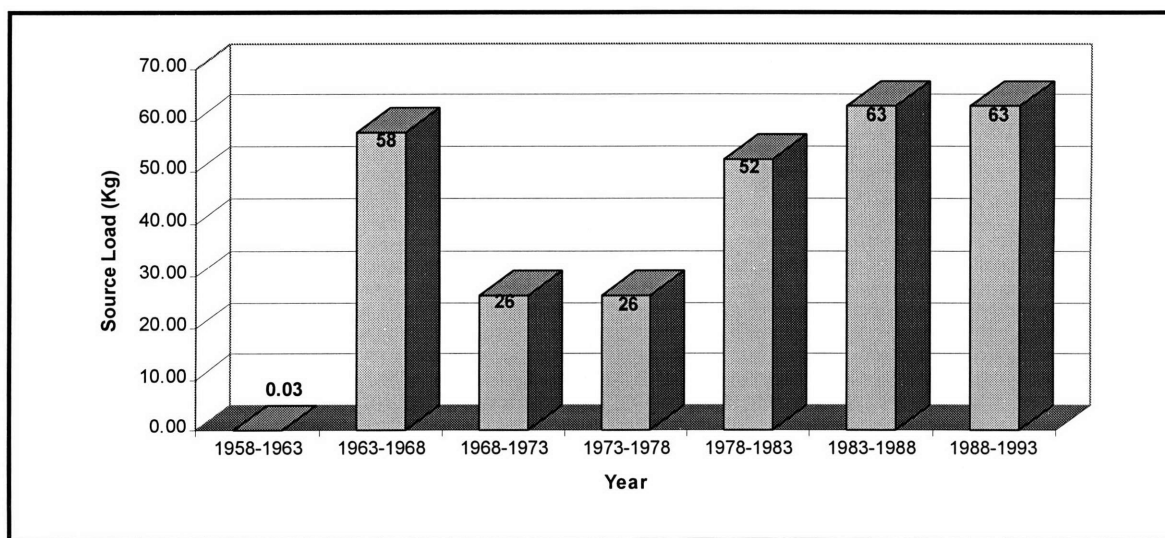


Figure B-1: Source Loadings for the CS-4 Model

*Dispersivity*

Garabedian et al. (1988) calculated dispersivities using the data obtained during the Ashumet Valley tracer test. The method of spatial moments was used to interpret the data; which was regarded by Gelhar et al. (1992) as having a high degree of reliability. Values of dispersivity obtained by Garabedian et al. (1988) are summarized in Table B-2.

Table B-2. Dispersivity values of the Ashumet Valley
Tracer Test (*Garabedian et al.*,1988)

| Dispersivity | Value |
|---|---|
| Longitudinal ($A_0$) | 3.15 ft |
| Transverse, horizontal ($A_{22}$) | 0.59 ft |
| Transverse, vertical ($A_{33}$) | 0.005 ft |

It must be noted that these values were obtained for a source with different dimensions as the CS-4 site. The overall test scale of the CS-4 site is larger, and the macrodispersivity should be modified (Gelhar, 1993). In addition, Rajaram and Gelhar (1995) conclude that dispersivities for transport over large scales are significantly influenced by the source dimensions. Using their two scale exponential model, the relative longitudinal dispersivity ($A_0^r$) is estimated to be 66 ft (Gelhar, 1996).

Transverse dispersivities are not affected, since their variability is not due to this phenomenon but to temporal variations of the hydraulic gradient's direction. This is a topic that is undergoing current research, and is beyond the scope of this work.

**Transport Model Results**

The code's capabilities allow concentration contours to be delineated. From this information the general size and shape of the contaminant plume was evaluated. The figures below (Figure B-2 to Figure B-4) show the graphical output of the model.
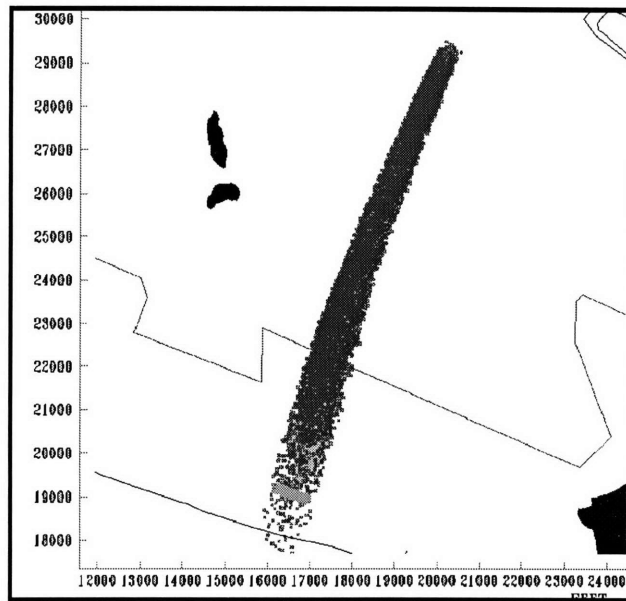
84

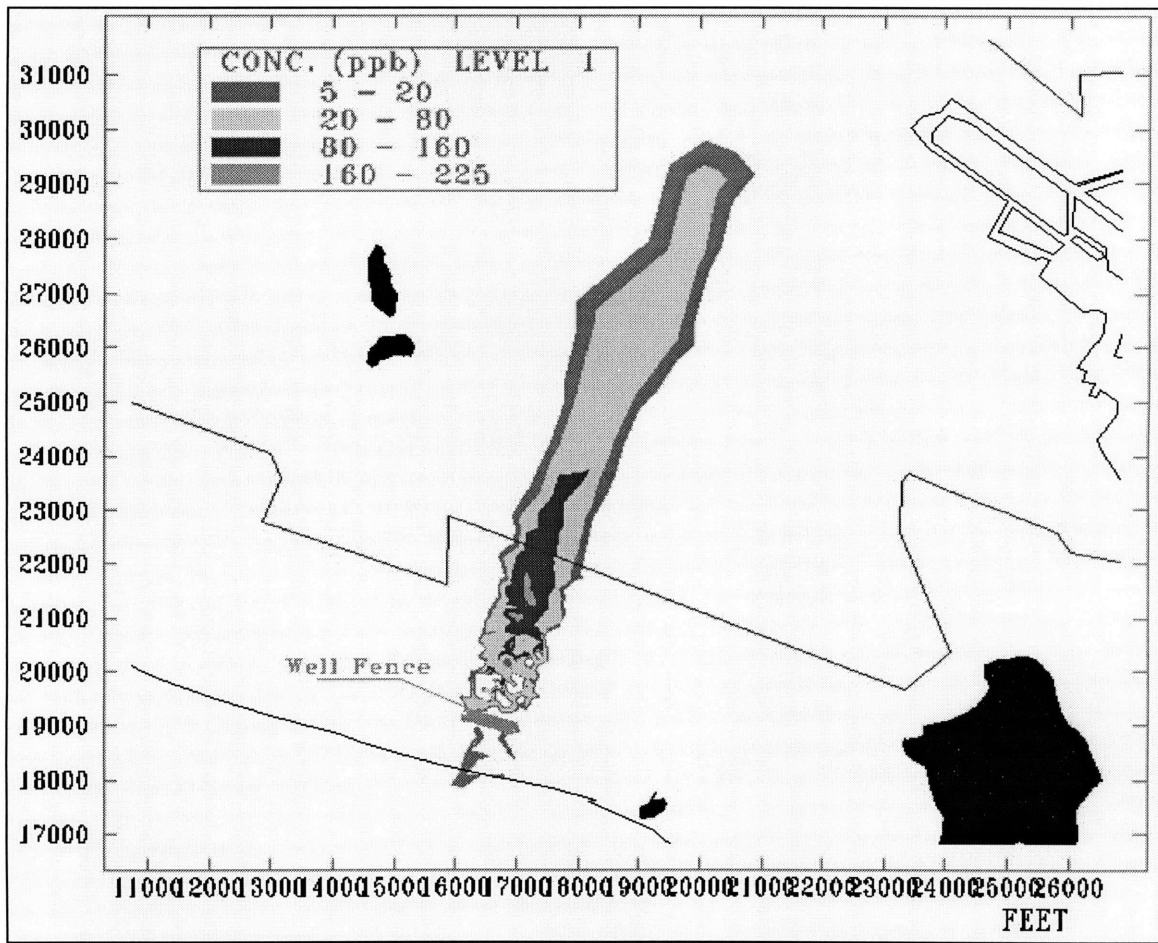Figure B-2: Distribution of Particles in the CS-4 Plume Simulation



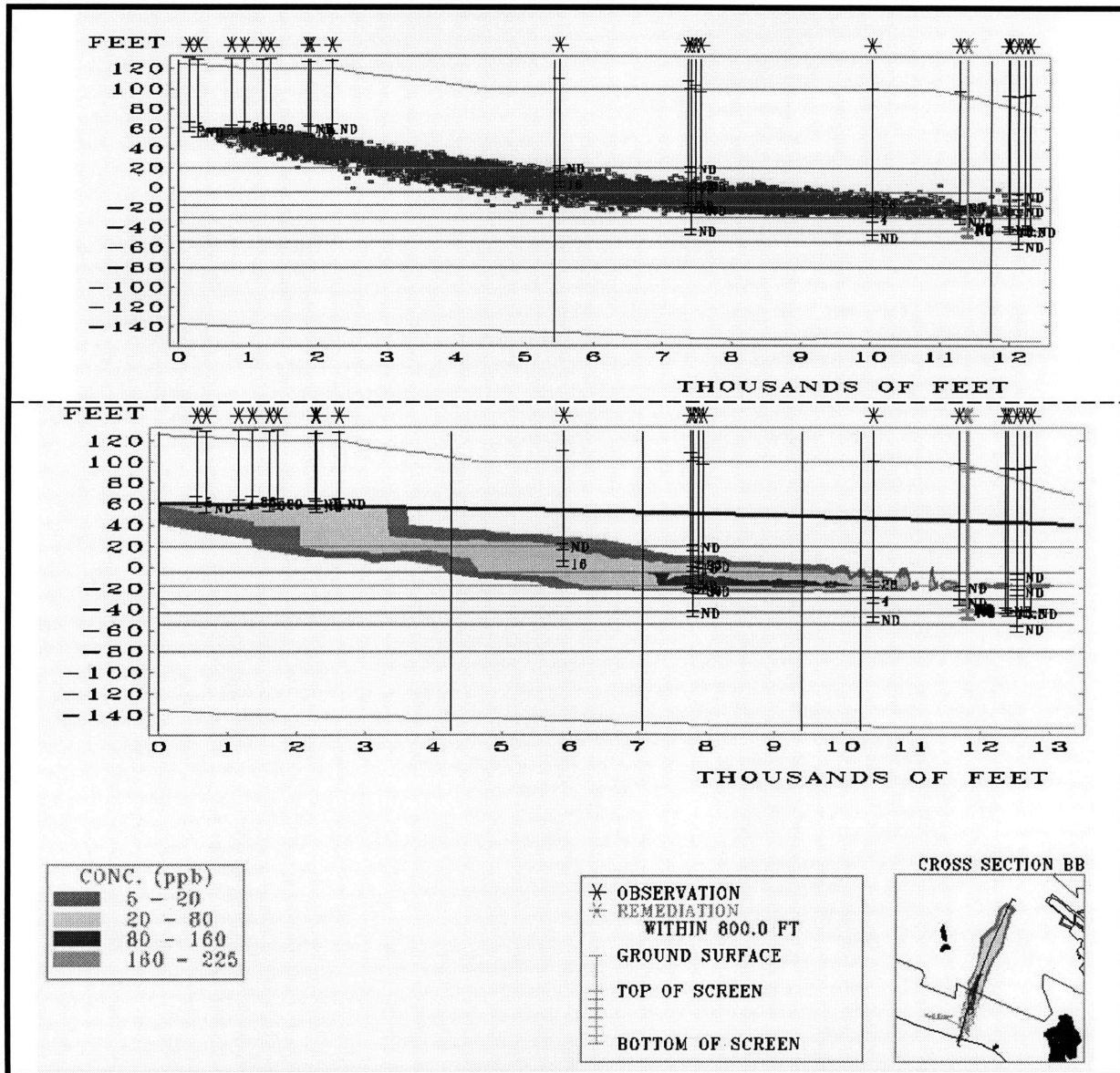Figure B-3:  Plan View of Maximum Concentration Contours

Figure B-4: North-South Cross Section of CS-4 Plume Showing Particle Distribution (top), Concentration Contours (bottom)

In general, the dimensions of the modeled plume are greater than the ones reported by ABB Environmental Services Inc.(1992b) (Table B-3). This result does not necessarily invalidate either plume interpretation. The plume defined by ABB Environmental Services Inc. (1992a) was developed from interpretation of the field observations. This simulation used field observations and site characterization data, applied to a calibrated natural conditions model

Table B-3: Dimension of Modeled Plume (at 5 ppb contour).

| Parameter | Value |
|---|---|
| Length | 3,840 m (12,600 ft) |
| Maximum Width | 640 m (2,100 ft)[*] |
| Average Width | 360 m (1,180 ft) |
| Maximum Height | 17 m (55 ft) |
| Average Height | 12 m (40 ft) |

[*] Maximum width is probably overestimated due to grid resolution

of the Cape Cod aquifer, and thus probably produces a more appropriate representation of the real plume. Nevertheless, there are many assumptions that are made and factors that come in when a computer model is constructed. Some of these, such as source dimensions and location, recharge, hydraulic conductivity distribution, and amount of data available may ultimately be the sources of the discrepancies between the modeled solution and the real plume. This suggests that site characterization should be improved in order to obtain a clearer understanding of the subsurface conditions.

**Transport Simulations**

The CS-4 plume model described above was used to simulate two different remediation alternatives. Both simulations were started with the plume as shown in Figure B-3 (in the simulation year 1993). These simulations attempted to forecast the clean-up times for the alternatives examined.

The first simulation was the no option alternative and therefore modeled the natural flushing of contaminants. The total time it took for all the particles to enter Coonamesett Pond was between 80 to 85 years. Thus, the model suggests that if the well fence had not been operating, the aquifer under the MMR would be "clean" approximately by the year 2075. Once the particles reached the pond, concentrations dropped notably, possibly due to dilution effects. This model could be used as the basis for further studies on surface water impacts.

The second simulation attempted to replicate the current pump and treat scheme used at the MMR. Thirteen extraction wells at the toe of the plume pump at a total rate of 140 gpm. The purpose of the simulation was to predict the time it would take to operate the pump and treat system continuously until concentrations reach acceptable levels. This occurred approximately 70 years after the simulation run started. This strongly suggests that a more economically efficient final remediation scheme should be put in place. It is interesting to note however, that some particles escaped the well fence and ultimately ended up in Coonamessett Pond. This is most probably be due to the fact the well fence is designed for an 800 ft (244 m) wide plume. López-Calva (1996) presents pumping schemes for the well fence in question.

## Modeling Pumping Schemes for Remediation

An aquifer test was carried out by E. C. Jordan (1990) and results are reported in the feasibility study for CS-4 area. This aquifer test was simulated using the model, in order to calibrate it under pumping conditions.

**Pumping Schemes for Remediation**

The first step in the design of a pump and treat system is to determine the quantity of groundwater that will need to be pumped from the aquifer. This contaminated water discharge for CS-4 was estimated to be 60 gpm. The minimum overall pumping rate of any remedial system simulated needs to consider this discharge as its minimum pumping rate.

*Analysis of the Capture Zones Under Different Pumping Schemes*

The particles which reach the well fence in the middle of pumping wells may or may not be captured, depending on the distribution of hydraulic head. Points of greater head value are formed at the midpoint between the pumping wells. This factor was important in the geometry for the capture zones as described below.

The results from the simulation of six wells non-uniformly spaced indicate that this option was less effective than the equally-spaced option. However, an efficient capture curve can be achieved with a proper combination of pumping rates.

*Flexibility of the current well fence*

The existing well fence was simulated first. A particle tracking simulation using 13 wells, pumping a total flow rate of 140 gpm (530 L/min), located 60 feet apart, as in the existing well fence, was run.
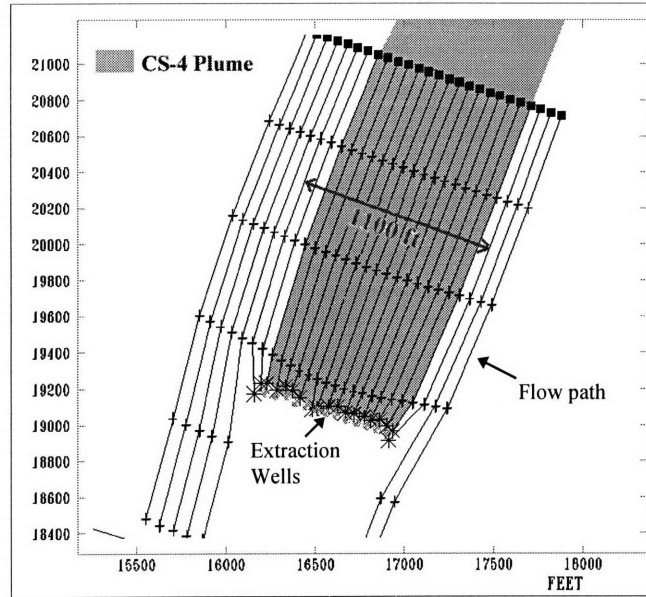
Figure B-5. *Capture curve simulation of the IRP well fence.*

The pumping rate and the number and spacing of wells in the existing well fence can be considered adequate (Figure B-5). In the horizontal view, a capture curve about 1,100 feet wide is observed. However, this horizontal view of the capture zone does not give information about the three-dimensional geometry. In order to obtain this information, a cross-sectional particle tracking was run. The particles were introduced into the modeled aquifer 1,500 feet upgradient of the well fence. The simulation was run and the starting points of the particles were plotted. The plot of the starting points is only a cross-section of the aquifer showing where the particles were at the beginning of a simulation. A second plot was made on top of the first one, showing only the starting points of the particles that, as a result of the pumping, were removed from the aquifer. In Figure B-6 a cross-sectional particle tracking for the simulation of the IRP well fence is shown. The larger dots can be interpreted as the cross-sectional area of the capture zone, 1,500 feet upgradient of the well fence.
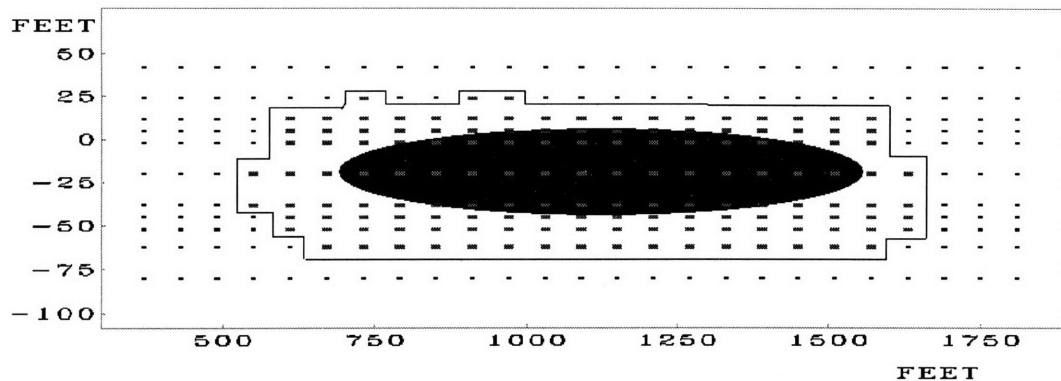
Figure B-6. Cross-sectional areas of the capture curve 1,500 feet upgradient of the 13-well system (IRP well fence).The capture curve is represented by the larger dots.

From the analysis of the cross-sectional area of the capture zone (Figure B-6), the vertical and horizontal effects of the pumping scheme were sufficient for the capture of the plume. The capture zone was calculated to be approximately 250 feet wider and 25 feet thicker than the CS-4 plume. The area of the ellipse formed by the plume is 31,400 ft$^2$. The area of the ellipse formed by the capture zone is about 64,800 ft$^2$. The cross-section of the capture zone is two times bigger than the cross-section area of the plume. This guarantee the removal of all contaminated water.

The simulated plume described earlier, is wider than the plume reported by E.C. Jordan (1990). The flexibility of the 13 well containment system, in terms of its response to different field conditions such as a wider plume was tested. In order to do this, simulations using the current well fence but increasing the pumping rate were made and the extent of the resulting capture zones were analyzed. Results indicate that pumping an overall discharge of 220 gpm, 13 wells will capture a plume about 50% bigger (in cross-sectional area) than that reported by E.C. Jordan (1990). However, if the plume is located deeper in the aquifer, the increase in pumping rate will not be effective, since the lower limit of the capture zone does not go deeper even for a pumping rate 75% larger than the original pumping rate. Placing the well screens deeper into the aquifer is a more effective way to contain a deeper plume than

increasing the pumping rate. The 220 gpm pumping rate, however, would not be enough to capture a plume with the dimensions of that simulated in this study. Higher pumping rates would be needed.

## *Prediction of an Alternative Pumping Scheme*

After the analysis of the current well fence of 13 wells, and the response of the aquifer to different pumping scenarios, the option of an alternative containment system was addressed. The different simulation runs for this purpose are presented in Table B-4.

Table B-4. Simulations to predict an alternative effective capture zone for CS-4 plume. Simulations were run according to the dimensions of the plume reported by E. C. Jordan (1989).

| Number of wells | Wells operating | Pumping rate (gpm) | Individual pumping rate (gpm) | Distance between wells (ft) |
|---|---|---|---|---|
| 8 | 13, 11, 10, 8, 7, 5, 3, 1 | 140 | 20 in the outside wells, and 16.7 at the rest of the wells | 102 |
| 8 | 13, 11, 10, 8, 7, 5, 3, 1 | 140 | 17.5 | 102 |
| 7 | 13, 11, 9, 7, 5, 3, 1 | 140 | 20 | 120 |
| 5 | 13, 10, 7, 4, 1 | 140 | 28 | 180 |

All simulations were run with schemes of equally-spaced wells, since in the six-well simulation it was clear that an option of non-equally spaced wells presents disadvantages compared with the uniformly-spaced options. The results in the cross-section capture zone generated by eight wells were very similar in terms of the shape of the capture zone and almost identical in terms of cross-sectional area, which is of about 64,800 ft$^2$.

Since fewer wells for a fixed pumping rate (140 gpm) may imply reduction in the operation and maintenance costs, the simulation of seven wells was performed. The resulting capture zone cross-section is illustrated in Figure B-7.
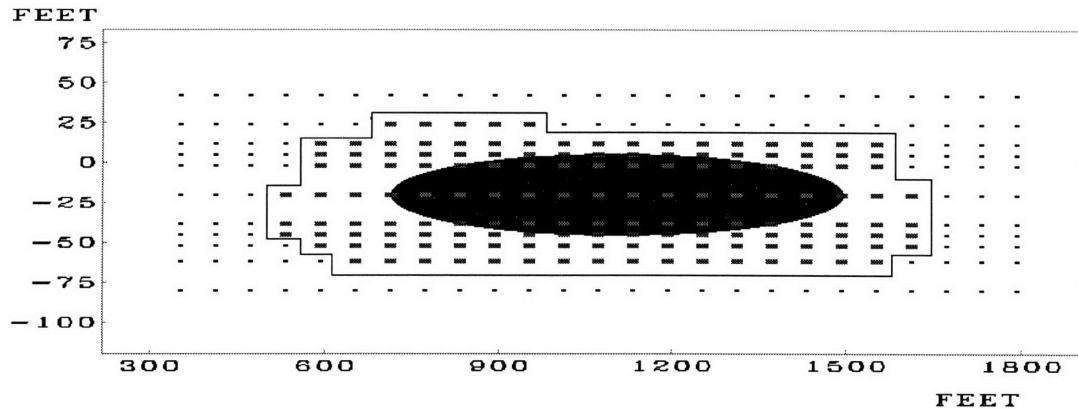


Figure B-7. Cross-sectional areas of the capture curve 1,500 feet upgradient of the 7-well system, pumping a total of 140 gpm. The capture curve is represented by the larger dots.

The area of the seven-well pumping strategy was also approximately 64,800 ft$^2$, which is the same as the 13 well and the previous eight well simulations. The seven well option is preferred over the eight-well option because both produced the same results, and in the eight-well system the wells had to be relocated. This relocation of wells would imply costs, not needed for the seven-well scheme.

For the simulation of five wells, pumping 140 gpm was not enough to contain the plume. Pumping rate had to be increased to offset the effect of well spacing. An increase of more than 40 % in pumping rate gave a capture zone of approximately 79,000 ft$^2$, which was greater than the one obtained from the other schemes. This capture curve, however was not effective in containing all the contaminants. No further simulations with five wells were run, since the greater capture zone from the five-well simulation implies the capture of a larger proportion of clean water, which makes this option less effective.

From the results of this study, no significant changes for the existing well fence and the seven-well alternative were observed. The seven-well alternative consists of wells located

120 feet apart, which is twice the distance between the wells in the current well fence. The pumping rate for each individual well was increased, although the overall pumping rate remained constant. The results show that the negative effect of increasing distance between wells was offset by the positive effect of increasing individual pumping rates.

In conclusion, the seven-well system may be a better option for the containment of CS-4. The operation and maintenance cost would be reduced and the capture of CS-4 plume would still be attained.

## *Bioremediation*

Bioremediation engineering is the application of biological process principles to the treatment of water or soil contaminated with hazardous substances (Cookson, 1995). *In situ* bioremediation provides a more effective and inexpensive approach  because it has the potential to: (1) completely degrade the contaminants (2) decrease the treatment time (3) use the subsurface as a bioreactor eliminating the need to pump the water to the surface for treatment; and (4) treat the contaminant "in place" causing minimal disturbance to the subsurface.

### General Considerations

Several requirements are necessary for the biochemical reactions to take place.  In order to optimize biodegradation, it is important to create an environment where all these factors are conducive to biodegradation and the limiting factor(s) are the contaminants.  This generally requires the addition of a substrate, oxygen,  and nutrients.

The engineering of the delivery systems and their control present the engineer more challenge than understanding the biochemical process.  The main problem with traditional applications of in situ bioremediation is that the delivery of the added agents is in the liquid form resulting

in displacement of the contaminated water and therefore inadequate mixing. This results to minimal biodegradation.

To overcome this problem, all agents of choice are added in the gaseous form. The injected gases move through the aquifer in discrete channels (Hayes, 1996) diffusing into the water on their way to the surface (carried by buoyancy). This creates a continuous source of the injected agent in the water.

**Cometabolic Oxidation and Reductive Dechlorination**

Xenobiotic compounds (i.e. foreign to natural biota) such as the chlorinated solvents found at the CS-4 site cannot be utilized by microorganisms for growth and energy (Buyer, 1992). The process of aerobic cometabolic oxidation has been proven to biodegrade TCE and other aliphatic compounds. Methane-oxidizing microorganisms have been found to be capable of cometabolically oxidizing TCE, DCE, and vinyl chloride (VC) in aerobic environments (Semprini et al., 1991).

PCE, however, can only be removed in anaerobic environments in a process termed reductive dechlorination. In this process, PCE loses a chlorine atom (turning into TCE) and achieves a lower oxidation state becoming susceptible to cometabolic oxidation.

**Process Design**

A successful bioremediation scheme for CS-4 should consist of an aerobic phase (for the treatment of TCE and DCE) and an anaerobic phase (for the treatment of PCE). This design was incorporated in three phases (Figure B-8).

Horizontal wells were utilized to inject the gases. The area of influence of the injected gases creates a biozone where the treatment takes place. It was assumed that a methane concentration of 1 mg/L and DO concentration of 10 mg/L can be achieved in the biozone.

## Phase 1

The objective of phase 1 was to stimulate microbial growth by injecting methane, air, and nutrients so a steady-state methanotrophic biomass (SSMB) concentration was reached.. Once SSMB was reached, phase 2 begins. It was calculated that it took about 5 days to create a SSMB of 5 mg/L.
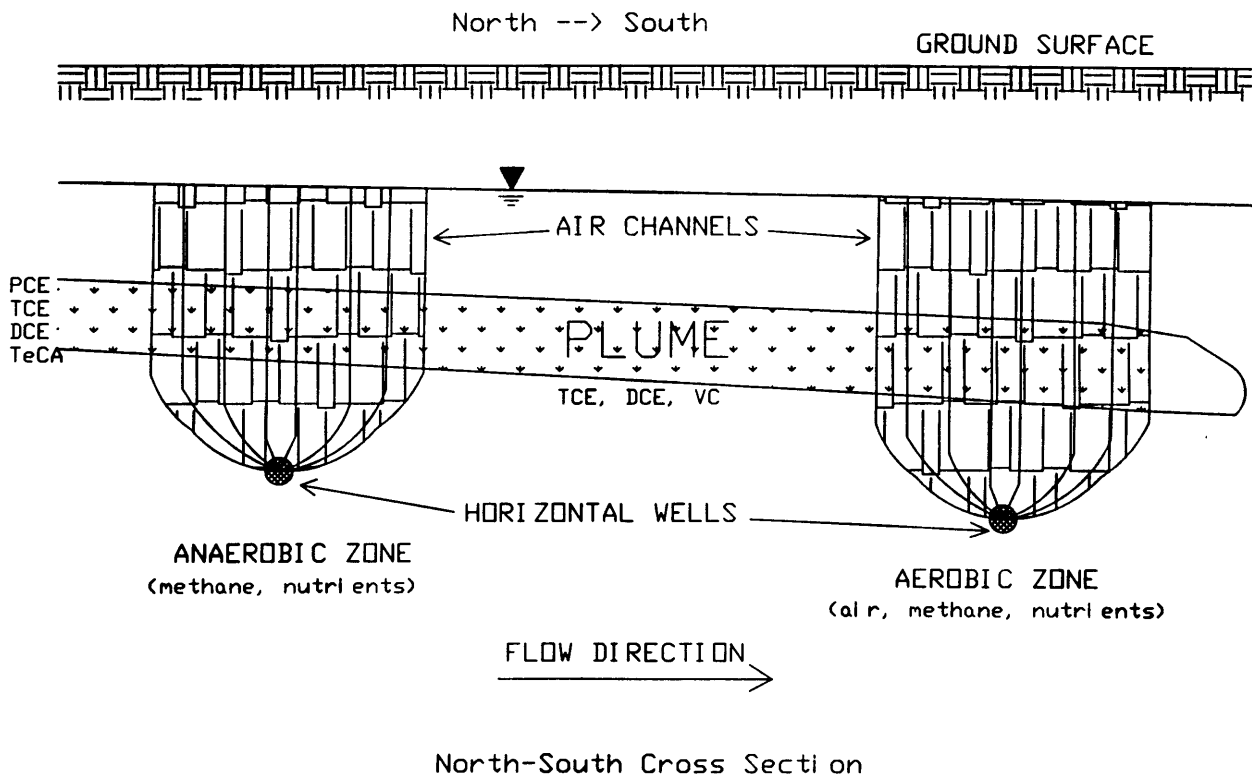
Figure B-8. North-south cross-section of the bioremediation scheme

## Phase 2

Phase 2 was an anaerobic phase. Its objective was the removal of PCE. The SSMB created in phase 1 was required as the electron donor in phase 2. To create an anaerobic

96

environment, the injection of methane and nutrients was continued while the injection of air was stopped. This exerted a biochemical oxygen demand to the aquifer turning it anaerobic in. The DO carried into the biozone by the water was consumed in just 2 ft. Collins (1996) calculated that under these conditions a 99 % removal of PCE can be achieved if adequate residence time is allowed. The residence time can be increased by the addition of horizontal wells which will extent the biozone by 200 ft per well. This corresponds to a residence time of 250 days per well since the seepage velocity is 0.8 ft/d (Lazaro, 1996).

**Phase 3**

Biozone II was placed downstream at a distance where no interference with biozone I would be possible (about 300 ft). In phase 3, methane and air were injected into the subsurface to stimulate cometabolic oxidation of TCE, DCE, and VC (VC be a by-product of phase 2). The resulting normalized concentrations of the contaminants are shown in Table B-5.

Table B-5. Resulting normalized concentration of TCE, DCE, and VC.

|  | TCE | c-DCE | t-DCE | VC |
|---|---|---|---|---|
| $k_{deg}$ (d$^{-1}$) | 0.014 | 0.068 | 1.36 | 1.36 |
| $t$ (d) | 250 | 250 | 250 | 250 |
| $Cc/Cc_o$ | 0.03 | 0 | 0 | 0 |

Figure B-9 shows the degradation of the contaminants within the biozone as a function of distance.
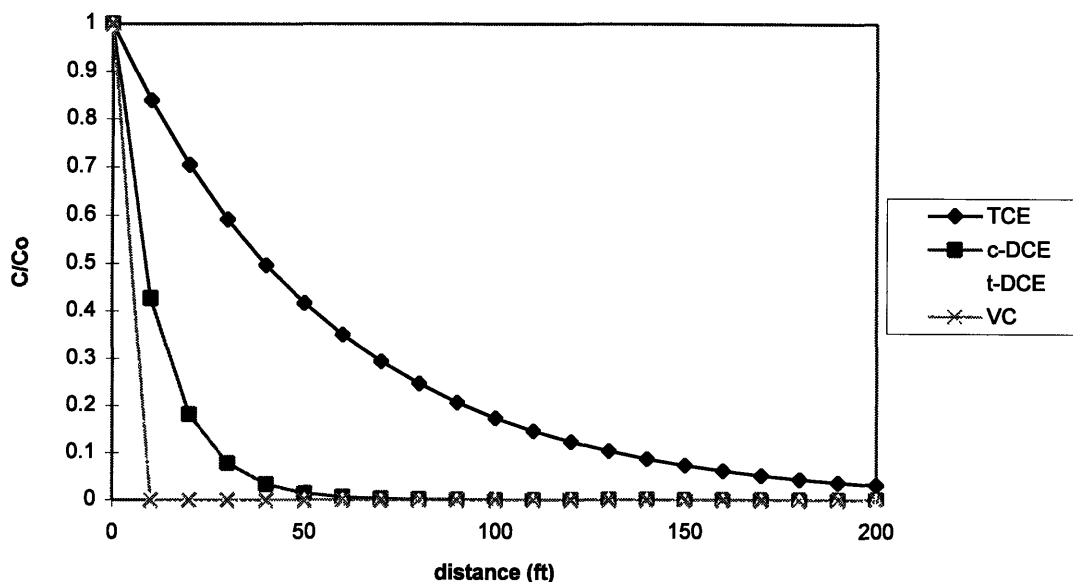


Figure B-9. Normalized contaminant concentrations as a function of distance

Discussion

A 97% removal of TCE, 99 % removal of PCE, and complete removal of the rest of the contaminants was achieved by this scheme. The conditions required (1.0 mg/L methane aqueous concentration and 10.0 mg/L) were assumed to be achievable in the field through proper engineering measures.

Field conditions are complex and hard to control. Factors affecting the in situ bioremediation of contaminants vary from site to site and caution must be given in the interpetation of the results obtained in this design. The contaminant removal calculated must serve for estimation purposes only. The mass transfer limitations and the spatial heterogeneity

encountered at a site create conditions that cannot be adequately predicted by theoretical approaches. A pilot test is necessary to predict the system's efficacy and determine final design parameters.

## *Aboveground Treatment Alternative*

Treatment of extracted groundwater by GAC is a proven and reliable technology (Stenzel et al., 1989). However, one of the disadvantages is that the operation and maintenance cost are relatively high. Principal cost contributions are due to the periodical exchange and reactivation of the exhausted carbon, when no more organic compounds can be adsorbed to it. Especially as successful pump and treat remediation requires operation of the system over a long period of time (for CS-4 estimated 70 to 75 years), this procedure results in considerable high costs.

It has been shown that the use of zero-valent iron is highly effective in promoting the breakdown of halogenated organic compounds in aqueous solution (Gillham, 1995). It was examined whether this emerging zero-valent iron technology could be combined cost-effectively with the existing GAC (Figure B-10). And whether this combination would be a feasible implementation at the CS-4 site.

Inflow

Zero-valent iron vessel

Adsorber 1

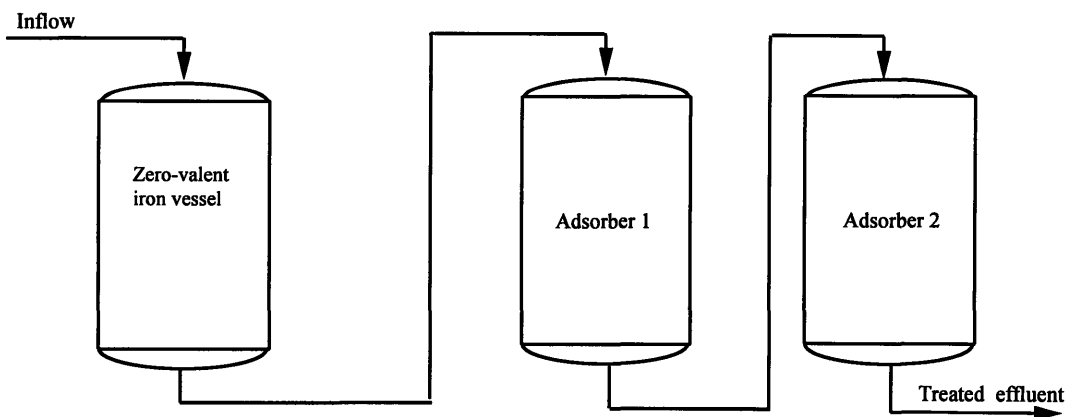Adsorber 2

Treated effluent

Figure B-10: Combination of Zero-Valent Iron with GAC (not to scale)

The basic concept is to pass the contaminated water through vessels filled with granular zero-valent iron before passing it through the GAC. The contact of the VOCs with the iron surface results in reductive dechlorination and thus destruction of the contaminants. Since this technology is innovative and only very little data regarding the efficiency and implementability is available, the GAC is added to the system as a polishing and safety unit. As a result of degrading the contaminants before they enter the GAC columns, the carbon does not get exhausted and therefore carbon reactivation costs can be reduced. Assuming the innovative zero-valent iron technology is feasible, a comparison between investment and savings indicates the worth of the concept.

**Scenarios of inflow concentration**

The size of the treatment facility depends on two major parameters: volumetric flowrate of water and the range of inflow concentrations of contaminants to be treated.

Since only about 20 samples determine the range of contaminant concentrations, the uncertainty is large. Furthermore, the proposed bioremediation system has never been tested in the field and therefore its efficacy as a treatment scheme is uncertain. In order to understand the behavior of the treatment system with respect to different inflow concentrations, the following calculations were made for two different scenarios. The two scenarios are thus defined as follows and summarized in Table B-6.

Scenario 1:    Assuming the maximum concentrations in the influent and bioremediation was not capable to diminish plume concentrations This scenario represents the worst case.

Scenario 2:    Assuming average concentrations prevailed throughout the whole plume, and no reduction by bioremediation.

Table B-6. Four scenarios for influent concentrations

| Contaminant of concern | Scenario 1: max conc. no bioremediation (ppb) | Scenario 2: average conc. no bioremediation (ppb) |
|---|---|---|
| PCE | 62 | 18 |
| TCE | 32 | 9.1 |
| 1,2-DCE | 26 | 1.1 |
| 1,1,2,2-TeCA | 24 | 6.8 |

**Combination of abiotic dehalogenation and GAC**

The net savings depend on the influent concentrations (Table B-7). For high concentrations (scenario 1), considerable savings can be expected, while at lower inflow concentrations (scenario 2-4), the costs are higher than the savings. Calculations are shown in Appendix F.

Table B-7. Net savings of the combination of GAC and zero-valent iron

| Scenario | Costs: Installation of zero-valent iron system and reduced carbon exchange cost (million $) | Savings: Present worth of carbon exchange cost (million $) | Net savings (million $) |
|---|---|---|---|
| Scenario 1 | 0.4 | 0.6 | 0.2 |
| Scenario 2 | 0.2 | 0.3 | 0.1 |

The results do not allow firm conclusions but require appropriate interpretation. Some assumptions made for the calculations are the following: steady inflow concentration, multi-component adsorption prediction, half-lives of the reductive dechlorination process, build-up of by-products, cost of the iron technology (vessels, construction etc.) and project lifetime. Therefore, the net savings should be seen as an order of magnitude estimate.

**Conclusions**

The results indicate that the combination of GAC with zero-valent iron could be feasible and result in a more economic aboveground treatment than the existing one. Furthermore, in the

near future the iron process is expected to progress significantly (Gillham, 1995). In order to better determine the effectiveness of this system, more data is required. A better estimation of the actual plume contamination and bench-scale or pilot testing of the zero-valent iron technology for the CS-4 site specific parameters are needed.

## *Risk*

### Introduction

There are numerous risks involved in any groundwater contamination or cleanup. Risk assessment is the identification and quantification of these risks and it is an objective scientific evaluation of the expected adverse health effects of exposure to potentially hazardous substances. Risk assessment consists of hazard identification, dose-response assessment, exposure assessment, and risk characterization. The data generated by a risk assessment is useful in determining the level of cleanup of a particular site, and in selecting the best remedial strategy for that site.

In the CS-4 plume, four hazardous substances are identified as primary contaminants in the groundwater: PCE, TCE, DCE and TeCA. Both carcinogenic and non-carcinogenic health effects are associated with these chemicals.

Risk calculations for carcinogens yield the probability of excess lifetime cancer from the exposure to the particular chemical. The cancer slope factor is needed for this calculation. This factor can be derived from dose-response relationships of the specific chemical. It represents the carcinogenic potency for the chemical. Carcinogenic risk can be calculated as follows (LaGrega, 1994):

$$Risk = CDI \times SF$$

where *CDI* is the chronic daily intake (mg/kg-day) and *SF* is the carcinogen slope factor (kg-day/mg). The acceptable range of carcinogenic risk (as set by EPA) is between $10^{-4}$ and $10^{-6}$ probability of excess lifetime cancer. However, the EPA uses a risk of $10^{-6}$ as a point of departure: risk above this level is acceptable only under extenuating circumstances.

Non-carcinogenic risk is quantified by a hazard index (HI). The hazard index is the ratio of the intake to the reference dose. Unlike carcinogens, non-carcinogens do not produce adverse health effects below a specific dose, or threshold. This dose or threshold is referred to as the reference dose. Non-carcinogenic risk is measured relative to this reference dose. A hazard index greater than 1.0 thus indicates that there is a possibility of adverse health effects. The hazard index, quantitatively, is (LaGrega, 1994):

$$HI = CDI / RfD$$

where *RfD* is reference dose (mg/kg-day) and CDI has been defined previously. The major pathways of human exposure to the contaminants are through direct ingestion of contaminated water, and through inhalation of vapors (volatilized during showering, etc.). The chronic daily intake (CDI) of the contaminants may be calculated directly from groundwater concentrations for the ingestion pathway. However, the concentration of inhaled vapor must be calculated via a "shower model", and the model of Foster and Chrostowski (1979) is used for this purpose.

**Results**

In the bioremediation scheme two cases are presented because the amount of TeCA that is degraded cannot be estimated due to lack of data. Two cases are then applicable: one wherein all TeCA is degraded, and one where all the TeCA remains in the groundwater. TeCA is more likely to be degraded, and a pilot study will be useful to determine the level of TeCA degradation. Table B-8 shows the resulting concentrations.

Table B-8. Contaminant levels after cleanup through bioremediation

| mg/L | | PCE | TCE | DCE | TeCA |
|---|---|---|---|---|---|
| Case 1 | Maximum | 0.6 | 1 | 0 | 0 |
| | Average | 0.2 | 0.3 | 0 | 0 |
| Case 2 | Maximum | 0.6 | 1 | 0 | 24 |
| | Average | 0.2 | 0.3 | 0 | 6.8 |

In the case where PCA may not be subject to bioremediation, as mentioned above, a pump and treat system is necessary to remove the PCA. In this case the resulting contaminant concentrations are tabulated below (Table B-9).

Table B-9. Contaminant levels after cleanup through bioremediation and pump & treat

| mg/L | PCE | TCE | DCE | TeCA |
|---|---|---|---|---|
| Maximum | 5 | 5 | 0 | 2 |
| Average | 5 | 5 | 0 | 2 |

Table B-10 summarizes the risks associated with the different treatment schemes. The data contained in the table can be viewed graphically in Figures B-11 and B-12. Both the table and the graph show that, following EPA guidelines, the plume must be remediated. Since it is possible to almost completely remove all contaminants from the groundwater, the best case for all remediation strategies involves no risk.

Table B-10. Risks associated with remediation schemes

| | Carcinogenic Risk | | Non-carcinogenic Risk | |
|---|---|---|---|---|
| | Maximum | Average | Maximum | Average |
| no action | $1.6 \times 10^{-4}$ | $4.5 \times 10^{-5}$ | $3.7 \times 10^{-1}$ | $9.2 \times 10^{-2}$ |
| pump and treat | $1.4 \times 10^{-5}$ | $1.4 \times 10^{-5}$ | $9.5 \times 10^{-2}$ | $3.8 \times 10^{-2}$ |
| bioremediation (1) | $3.1 \times 10^{-7}$ | $8.9 \times 10^{-8}$ | $5.7 \times 10^{-3}$ | $1.6 \times 10^{-3}$ |
| bioremediation (2) | $1.5 \times 10^{-4}$ | $4.2 \times 10^{-5}$ | $5.7 \times 10^{-3}$ | $4.5 \times 10^{-3}$ |
| combination (bio 2) | $1.3 \times 10^{-5}$ | $1.3 \times 10^{-5}$ | $5.7 \times 10^{-3}$ | $1.6 \times 10^{-3}$ |

Figure B-11.  Carcinogenic risk

**Carcinogenic Risk**



Figure B-12.  Non-carcinogenic risk

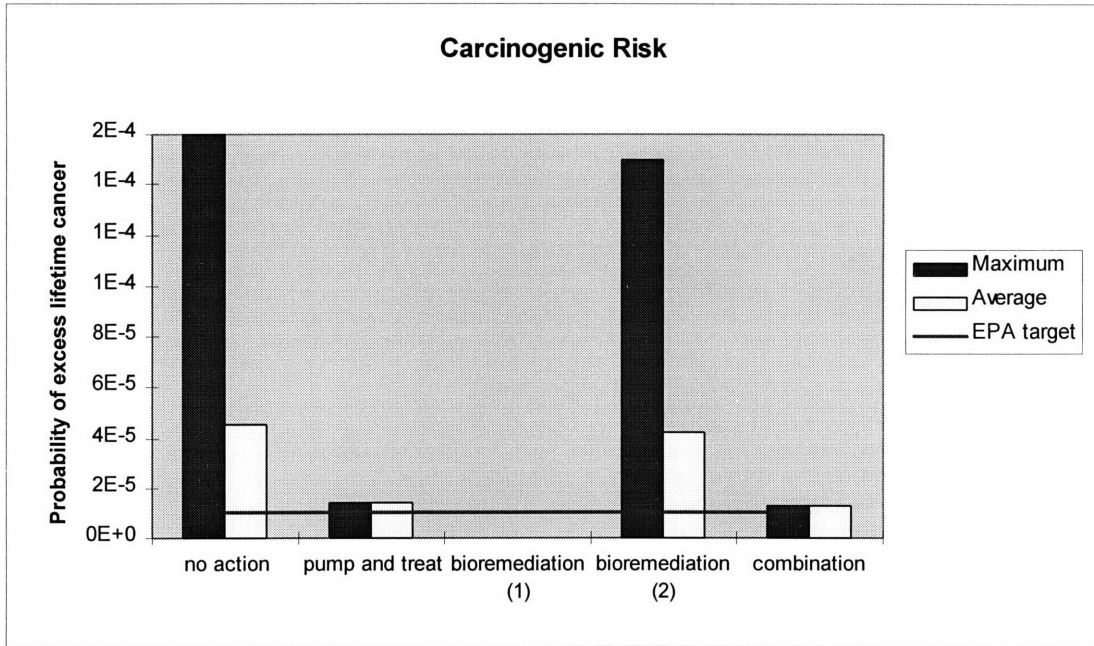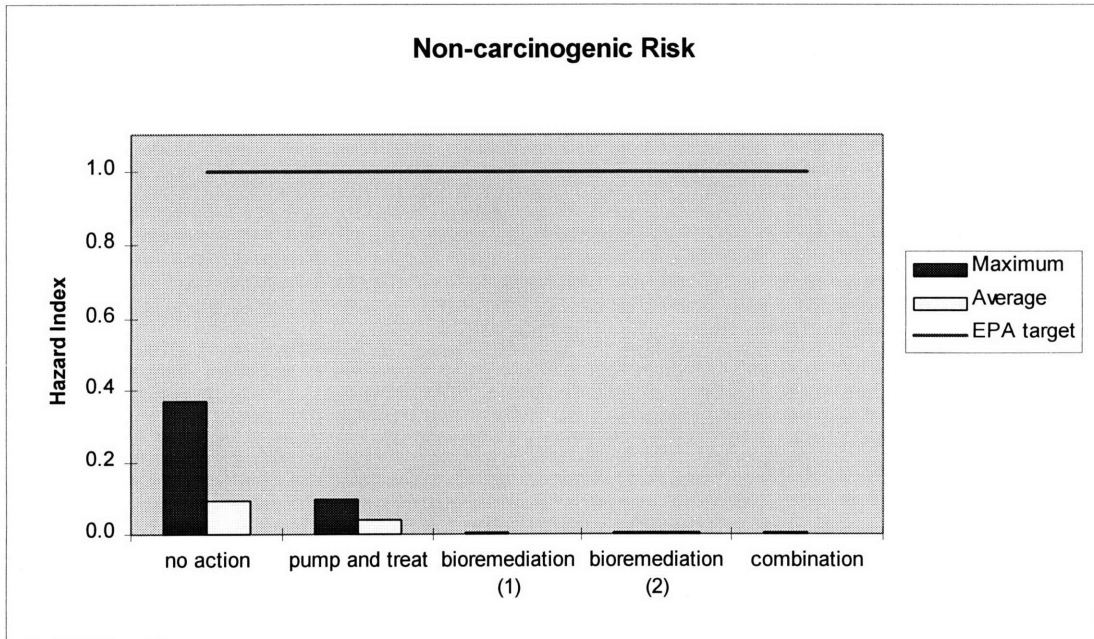**Non-carcinogenic Risk**

## Discussion

The process of calculating risk involves the use of approximations and conservative assumptions. Thus the risks calculated are generally estimates. Keeping in mind that the primary purpose of risk assessment in this project is the comparison of alternative remediation strategies, these values then become meaningful. All the uncertainties inherent in the calculations apply to each remediation scenario, and therefore the risks can be compared across remediation strategies. The assessment can also show which of the contaminants poses the greatest risk.

It is apparent that simply allowing the plume to proceed unabated can result in unacceptable risk, at least from a regulatory standpoint. In addition, the calculated risks do not take into account any potential ecological risk if groundwater contaminants are discharged into surface waters such as Coonamessett Pond.

From Figure 4-12 it can be seen that all calculated non-carcinogenic risks are well below the Hazard Index limit of 1.0, and do not seem to pose a threat to human health. Carcinogenic risks, however, vary up to two orders of magnitude from case to case. Figure B-12 shows that in contrast to non-carcinogenic risks, carcinogenic risks for the no action alternative are above the limit. The various treatment schemes yield risks within acceptable range, except for the bioremediation case where TeCA is assumed to resist degradation. In this case a pump and treat system is necessary to remove TeCA.

From a risk point of view, any of the alternatives which reduce the risk to permissible levels is acceptable. Therefore the pump and treat system, the bioremediation scheme (assuming satisfactory TeCA degradation), and a combination of the two are acceptable. However, the one which realistically yields the lowest risk, namely the combination, is the recommended one. The bioremediation scheme which assumed complete TeCA removal results in the lowest calculated risk, but if this is true then addition of pump and treat system will lower the risk even more. Aside from the lowered risk, the pump and treat system serves as a back-

up to the bioremediation, especially during the start-up period. The combination assures the satisfactory removal of the groundwater contaminants.